NITRATE IN COAL WASTE ROCK DUMPS, ELK VALLEY, BRITISH COLUMBIA, CANADA

A Thesis Submitted to the College of
Graduate Studies and Research
In Partial Fulfillment of the Requirements
For the Degree Master of Science
In the Department of Geological Sciences
University of Saskatchewan
Saskatoon

By
Fazilatun Nessa Mahmood

PERMISSION TO USE

In presenting this thesis in partial fulfillment of the requirements for a Postgraduate degree from the University of Saskatchewan, I agree that the Libraries of this University may make it freely available for inspection. I further agree that permission for copying of this thesis in any manner, in whole or in part, for scholarly purposes may be granted by the professor or professor who supervised my thesis work or, in their absence, by the Head of the Department or the Dean of College in which my thesis work was done. It is understood that any copying or publication or use of this thesis or parts thereof for financial gain shall not be allowed without my written permission. It is also understood that due recognition shall be given to me and to the University of Saskatchewan in any scholarly use which may be made of any material in my thesis.

Requests for permission to copy or to make other use of material in this thesis in whole or part should be addressed to:

Head of the Department of Geological Sciences
University of Saskatchewan
114 Science Place
Saskatoon, Saskatchewan
Canada
S7N 5E2

ABSTRACT

Explosives used for blasting during mining operations contain nitrogen (N) compounds. The release of N from blasting residuals can result in elevated nitrate (NO_3^-) concentrations in freshly blasted waste rock, which can be subsequently leached from waste rock dumps. The distribution and leaching of NO_3^- through coal waste rock (rates and efficiencies) in the Elk Valley, British Columbia, Canada were studied using multiple datasets of NO_3^-, collected from pre-blast and fresh-blast rock, an unsaturated waste rock dump deposited between 1982 and 2012, and humidity cell (HC), and leach pad (LP) experiments. Chemical analyses showed NO_3^- concentrations in fresh-blast rock (27.6±47.4 mg/kg; n=36) to be greater than pre-blast rock (0.20±0.10 mg/kg; n=22). $\delta^{15}N\text{-}NO_3^-$ and $\delta^{18}O\text{-}NO_3^-$ analyses confirmed that the source of NO_3^- in the dump was the N used in the explosives. Laboratory aqueous leach tests on fresh-blast rocks showed the mass of N released from fresh waste rock equated to 3.4% N loss from the blasting residuals. $\delta^{15}N\text{-}NO_3^-$ and $\delta^{18}O\text{-}NO_3^-$ data suggested limited to no denitrification occurred in the unsaturated dump. Total NO_3^--N mass released from humidity cells, leach pads, and boreholes indicated the leaching efficiency (E_L) of NO_3^- to be scale dependent at about 20, 40 and 80%, respectively. Scale dependency of E_L suggested that the findings from smaller scale experiments (HCs and LPs) are not applicable to the field-scale dump, but can be valuable for understanding the flushing mechanism of NO_3^- from the dump. Since 1982 the total NO_3^--N mass flushed from the WLC dump was estimated to be about 1.1×10^6 kg.

ACKNOWLEDGEMENT

First of all, I would like to thank almighty God for the completion of my thesis.

This dissertation is a compilation and culmination of research works collaborated with faculties, scientists, and Teck Coal Limited whose help and support were very helpful.

I would like to thank my advisors Dr. M. Jim Hendry and Dr. S. Lee Barbour for their inspiration, cordial and perceptive guidance, and constructive criticism and suggestions during my research work.

I am grateful for the participation of my committee members: Dr. Matt Lindsay, Dr. Bruce Eglington, and Dr. Richard E. Farrell for their advice and suggestions.

A special thanks to Erin Schmeling, Fina Nelson, and Virginia Chostner for their laboratory assistance regarding all aspects of geochemical data in this thesis.

I acknowledge Teck for their financial contribution.

I thank Dr. Chris Kennedy from SRK Consulting for providing geochemical data from humidity cell and leach pad experiments.

Finally, a special thanks to my family for supporting me during my study and providing moral support.

TABLE OF CONTENTS

LIST OF FIGURES

LIST OF TABLES

1. INTRODUCTION AND LITERATURE REVIEW

1.1. Introduction and Objectives

Nitrate (NO_3^-) is common in groundwater and surface water. It is generally derived from diffuse or point sources associated with the use of fertilizer or biological waste from agriculture or municipal sources (Power and Schepers, 1989; Hallberg and Follett, 1989; Seiler et al., 1999; Wakida and Lerner, 2005). Elevated concentrations of NO_3^- can lead to health risks in humans (Comly, 1987; Johnson et al., 1987; Kross et al., 1993), and eutrophication of surface waters (Durand et al., 2011; James et al., 2005; Jeppesen et al., 2005; Van der Molen et al., 1998). The maximum drinking water concentration is established at 10 mg NO_3^--N/L (WHO, 2004; Health Canada, 2014; U.S. EPA, 2009. Nordin and Pommen (2009) set the average and maximum concentrations for fresh water aquatic life at 3 and 33 mg NO_3^--N/L, respectively.

An important but less studied source of NO_3^- is nitrogen (N) based explosives such as those used to blast rock during mining operations. The primary blasting agent used is ammonium nitrate (NH_4NO_3) mixed with fuel oil, often referred to as ANFO (94-98% NH_4NO_3 + 2-6% fuel oil) (Bailey et al., 2013; Ferguson and Leask, 1988; Pommen, 1983). The scale of ANFO usage by the coal mining industry is reflected by the fact that it purchased 69% of all explosives sold in the United States in 2013 (USGS, 2013). Ammonium Nitrate (NH_4NO_3) is highly soluble in water and dissociates into NO_3^- and NH_4^+. In an alkaline environment, NH_4^+ further dissociates to NH_3. The release of NO_3^- and NH_3 from explosives during mining operation is usually attributed to NH_4NO_3 spillage or incomplete detonation and subsequent dissolution (Pommen, 1983; Cameron et al., 2007; Bailey et al., 2013). In spite of the widespread use of ANFO, detailed studies of the distribution and geochemical controls on NO_3^- in blasted and stockpiled waste rock are few (Pommen, 1983; Ferguson and Leask, 1988; Bailey et al., 2013). Further, we are aware of no studies that addressed the long-term leaching of ANFO derived NO_3^- from waste rock dumps, nor the hydrogeochemical controls on blasting derived NO_3^- and NH_3 within waste rock dumps.

The Elk Valley watershed, British Columbia, Canada is a major source of steelmaking coal in Canada (Goodarzi et al., 2008) (Figure 1a). Coal mining in the Elk Valley began in 1897, with large-scale open-pit coal mining beginning in the late 1960s. Currently, there are five open-

pit coal mining operations in the valley: Coal Mountain Operations (CMO), Elkview Operations (EVO), Line Creek Operations (LCO), Greenhills Operations (GHO), and Fording River Operations (FRO) (Figure 1b). Mining at CMO, EVO, LCO, GHO, and FRO commenced in 1985, 1969, 1982, 1982, and 1972, respectively (Teck Resources Limited, 2014). All mines use conventional open pit drill and blast methods, and truck and shovel technology. These operations resulted in the generation of about 4.7 billion bank cubic meters (BCM) of waste rock by 2010 (Teck EVWQP Annex D.4, 2014), most of which is deposited in dumps. These dumps were typically constructed by end dumping on mountain slopes, resulting in average dump thicknesses of more than 100 m. The majority (95-100%) of this waste rock consists of interburden siltstones and mudstones and thin, un-minable coal seams of the Mist Mountain Formation (Gibson, 1981; Vessey and Bustin, 2000).

During the early 1960s and 1970s, mean background nitrogen (NO_3^--N + NO_2^--N) concentrations measured in the Elk River south of Sparwood (Figure 1b) were < 0.01 mg/L (Clark et al., 1984; McDonald, 1987). Rising trends in concentrations of contaminants of interest (CIs), including NO_3^-, were observed in the river since early 1980's (Pommen, 1983; McDonald, 1987; Ferguson and Leask, 1988). Ferguson and Leask (1988) attributed the source of NO_3^- to N-based explosives used in rock blasting. The increasing levels of NO_3^- in the Elk River with time were positively correlated with the volume of waste rock produced (Strategic Advisory Panel on Selenium Management, 2010).

This study hypothesized: i) NO_3^- in the coal waste rock dumps is derived from blasting and/or oxidation of blasting residuals in the waste rock dump; and ii) in oxic, unsaturated waste rock dumps, NO_3^- acts as a conservative tracer, and consequently, can be used to evaluate flushing behavior of water through the dump. The objectives of the current study were to: i) characterize and quantify the source(s) of NO_3^- in waste rock dumps in the Elk Valley, British Columbia; ii) define the geochemical controls exerted on NO_3^- within the dump; and iii) characterize the long-term leaching of the NO_3^- from the dump. The objectives were attained by analyzing waste rock samples collected from the parent (pre-blasted) rock, fresh-blasted (less than 10 d old), and aged waste rock from existing dump (deposited between 1982 and 2012). The evolution of NO_3^- release in porewater from humidity cell (HC) and leach pad (LP) experiments were also compared to the NO_3^- concentrations in water samples collected from a rock drain located at the base of a dump.

The current study is part of a multi-disciplinary research program established in 2012 to improve the understanding of the origin, fate, and transport of CIs derived from dump in the Elk Valley. Such knowledge is critical to the evaluation of present-day and future CI releases from the dump and to identify potential measures to control the loading of CIs to the environment. As a part of this research program, recent geochemical studies characterized the source reservoirs of selenium (Se), arsenic (As), iorn (Fe), and sulfur (S) in the dumps of Elk Valley (Hendry et al., 2015; Biswas et al., 2016; Essilfie-Dughan et al., 2016) and water migration through the dumps (Barbour et al., 2016).

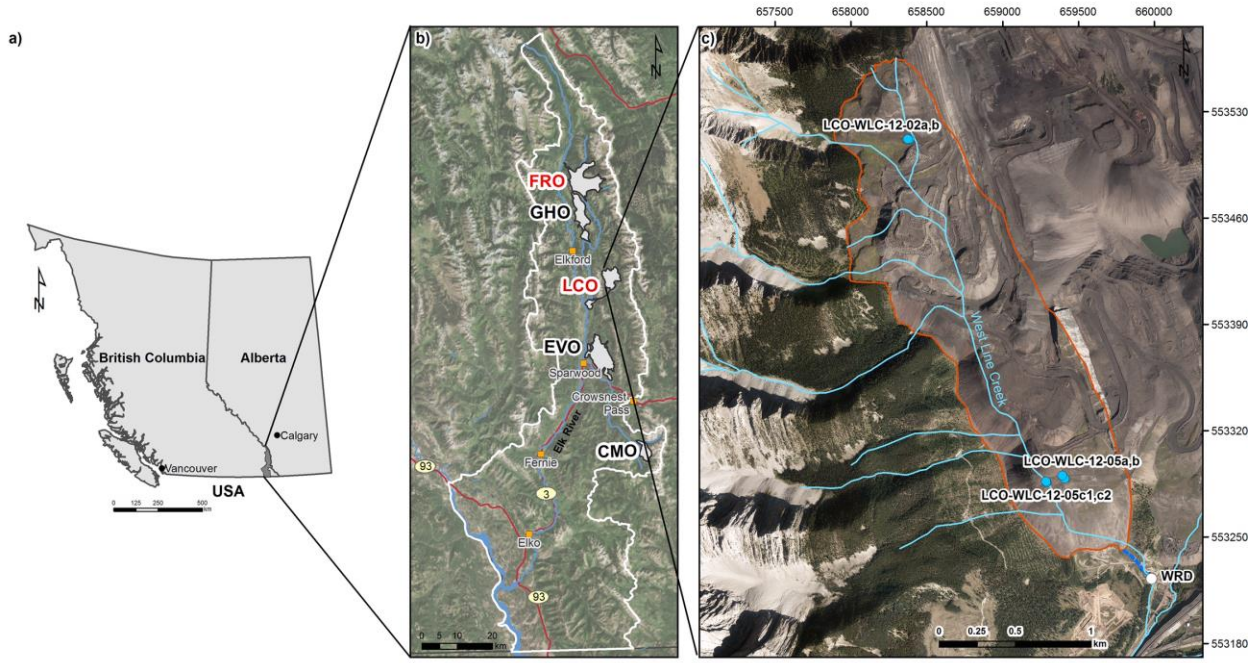

Figure 1. Location map of (a) Elk Valley, British Columbia, Canada; (b) Regional coal mining operations (FRO, GHO, LCO and EVO, and CMO) in the Elk Valley. The limits of the Elk River watershed boundary in Canada are delineated with a solid white line. Fresh-blast samples were collected from FRO. Pre-blast and waste rock samples (1982-2012) were collected from LCO; and (c) West Line Creek (WLC) catchment area with the footprint of the LCO-WLC dump delineated by a solid orange line. The rock drain formed along the pre-existing West Line Creek is conducted downstream from the toe by an underground culvert (dashed blue line) to the sampling location (WRD, solid white circle). Borehole locations are identified by blue circles.

1.2. Literature Review

The use of N (nitrogen) based explosives in open pit mining results in large volumes of waste rock that contain residual NO_3^- as a result of undetonated explosives (Bailey et al., 2013; Ferguson and Leask, 1988; Pommen, 1983). These waste rock deposits also serve as potential sources of other CIs due to the oxidation of waste rock materials. Blasting significantly modifies rock properties (texture, porosity, permeability, etc.), and lead to the creation of different physicochemical environments within the waste rock dump. Thus, the physical, chemical and microbial processes within fresh-blast rock are different from naturally occurring pre-blast rocks. In addition, geochemical processes such as redox reactions, dissolution, etc., and coupling among these processes play an important role in the mobilization of both anthropogenic and naturally occurring substances.

1.2.1. Explosives and Initial NO_3^--N Concentration (Nloss)

The primary blasting agent generally used in the mining industry is ammonium nitrate (NH_4NO_3) mixed with fuel oil (ANFO; 94-98% NH_4NO_3 + 2-6% fuel oil) (Bailey et al., 2013; Ferguson and Leask, 1988; Pommen, 1983). A major drawback of ANFO is its hygroscopic nature. Moisture contents as low as 5% can cause it to lose its effectiveness, resulting in detonation failure (Pommen, 1983). The lack of water resistance of ANFO led to the development of slurry explosives in the mid 1950's which were considered to be water resistant under wet blasting conditions. The slurry is a mixture of oxidizers (NH_4NO_3, $NaNO_3$) and fuels (fuel oil, gilsonite, sulphur, and aluminum) in an aqueous medium (15% water) thickened with gaur gum (Pommen, 1983). In recent years, emulsion is widely used for blasting due to the inherent contamination problems associated with slurry use. Emulsion is generally mixed with ANFO and contains 20-30% total N (Egly and Neckar, 1964). It is made of tightly packed small droplets of supersaturated NH_4NO_3 aqueous solution surrounded by a mixture of immiscible fuel oils and wax. Therefore, it is considered to be more effective at reducing N release in the mining environment (Young, 2007). Depending on blasting efficiency, most of the nitrogen is believed to be lost to the atmosphere as gaseous forms (N_2O, Vyazovkin et al., 2001; Sinditskii et al., 2005), and the remainder stays in the waste rock. Residual undetonated nitrogen, often referred

to as initial NO_3^--N concentration or nitrogen loss (N loss), is subject to leaching and can be estimated by measuring the total mass of N in the effluent (Pommen, 1983; Bailey et al., 2013).

Pommen (1983) studied the effect of N based explosives in the mining aqueous environment at Fording River, BC, operated by Fording Coal Limited. This study showed that the use of explosives had the potential to deteriorate water quality due to the high concentration of NO_3^- and NH_3. One of the key findings of this study was that the predominant use of slurry explosive under wet blasting condition appeared to worsen N loss from the mine. Pommen (1983) also reported ~1% of the ANFO and 6% of slurry N loss from the explosives used at the Fording Coal mine during 1979-80. As a result, NO_3^-, NO_2^-, and NH_3 often exceeded the water quality criteria for drinking water and aquatic life under low flow conditions (winter) in the Fording River.

Ferguson and Leask (1988) examined 15 sets of annual explosives data from 1980 to 1986 to evaluate Pommen's (1983) findings and investigate N loss from five surface coal mines (Byron Creek, Westar-Greenhills, Fording, Crows Nest Resources-Line Creek and Westar-Balmar) located in southeastern BC. Based on the proportion of slurry explosive used under different blasting conditions (wet or dry), a quantitative framework was provided to estimate N loss as a function of ANFO and slurry used, and moisture level in the blasting environment. This study also reported 0.1 and 4.3% N loss from <1% slurry used in dry blasting condition and 20-70% slurry in wet blasting condition after one year of waste deposition, respectively (Ferguson and Leask, 1988). Their study does not estimate the total soluble N present in the waste rock after blasting.

Bailey et al. (2013) further reported N loss at multiple scales ranging from laboratory leach test to large scale test piles at Diavik Diamond Mine, Northwest Territories, Canada operated by Diavik Diamond Mines Inc. Bailey et al., (2013) estimated a total N loss of 5.4% at the laboratory scale, and 2 to 12% from the Diavik waste rock test piles.

The fate of nitrogen species, once released into the surrounding waste rock, depends largely on the redox conditions. Residual undetonated NH_4NO_3 in the waste rock dump is readily soluble in water and will dissociate into nitrate (NO_3^-) and ammonium (NH_4^+) (Revey et al., 1996). The NH_4^+ itself can dissociate to ammonia (NH_3) in an alkaline environment (Clark et al., 1984), which later can be oxidized to NO_3^- by nitrifying bacteria (Sawyer and McCarty, 1967). Nitrification, the microbial transformation of NH_4^+ to NO_2^- and NO_3^-, is a very important

oxidation process in the nitrogen cycle (Seitzinger, 1990; Sloth et al., 1992) and is further discussed in Section 1.2.7.

Under oxic conditions, NO_3^- is stable and persists in solution and is not subjected to absorption by soil particles (Baalsrud and Baalsrud, 1954). Nitrate is a highly soluble and mobile anion that is readily transported with recharging water through oxic soils to groundwater and surface water. Dissolved inorganic nitrogen can have one of four oxidation states (N: +V, N: +III, N: 0, and N: -III) which could occur as NO_3^-, NO_2^-, N_2, and NH_3 depending on the redox condition of the system.

1.2.2. Environmental Isotopes

Stable environmental isotopes are measured as the ratio of the two most abundant isotopes of a given element (e.g., N, O, Se, S, Zn) and widely used to trace the source and fate of CIs. Due to fractionation processes, isotopes of any particular element often develop unique isotopic compositions (ratio of heavy to light isotope) that may be indicative of their source, or the processes that formed them.

Stable isotope compositions are normally reported as δ (i.e., 'delta') values. The symbol δ denotes the difference between the measured ratio of the sample and standard over the measured ratio of the standard. The symbol δ tells how much the sample deviates from the standard. δ values are reported in units of parts per thousand, denoted as ‰ or permil relative to a standard of known composition, and are calculated using the following equation:

$$\delta (‰) = [(Rx / Rs) - 1] \times 1000 \quad \text{……} \quad (1)$$

where,

Rx= Ratio of the heavy to light isotope of the sample (e.g., $^{15}N/^{14}N$, $^{34}S/^{32}S$)

Rs= Ratio of the heavy to light isotope of the standard.

Isotopic compositions of materials analyzed are usually reported relative to international reference standards. During analyses, samples are analyzed at the same time with an international reference standard, or with some internal laboratory standard that has already been calibrated relative to the international standard.

1.2.3. Nitrogen and Oxygen Isotopes

Nitrogen has two naturally occurring stable isotopes: ^{14}N and ^{15}N. The most abundant nitrogen isotope in the atmosphere is ^{14}N (99.6337%), and the remainder is ^{15}N (0.3663%). The wide range of oxidation states of nitrogen compounds (+5 to -3) results in a range of isotopic composition. Oxygen has three stable isotopes: ^{16}O, ^{17}O, and ^{18}O. The relative abundance of these three isotopes in the atmosphere are 99.759%, 0.037%, and 0.204%, respectively. Stable isotope ratios of ^{15}N and ^{18}O are expressed by the following equations:

$$\delta^{15}N_{sample}\ (‰) = [\{(^{15}N/^{14}N)_{sample} / (^{15}N/^{14}N)_{standard}\} - 1] \times 1000 \quad \ldots\ldots\ldots\ldots\ldots\ldots\ldots\ldots (2)$$

$$\delta^{18}O_{sample}\ (‰) = [\{(^{18}O/^{16}O)_{sample} / (^{18}O/^{16}O)_{standard}\} - 1] \times 1000 \quad \ldots\ldots\ldots\ldots\ldots\ldots\ldots\ldots (3)$$

$\delta^{15}N$ values are normalized against values of the IAEA (International Atomic Energy Agency) ammonium sulfate reference materials N-1 (0.4±0.2‰; ± represents one standard deviation), N-2 (30.2±0.2‰) and IAEA-NO_3^- (4.7±0.2‰), respectively. $\delta^{18}O$ values are referenced against the standard SMOW (Standard Mean Ocean Water), or the equivalent standard VSMOW (Vienna Standard Mean Ocean Water).

1.2.4. Sources of NO_3^-: Dual Isotope Approach

The isotopic composition of nitrogen in various NO_3^- sources such as atmospheric N_2, soil, chemical fertilizers, and manure is usually different and shows a wide range. As a result, stable nitrogen (N) isotope data of NO_3^- ($\delta^{15}N$-NO_3^-) have been regularly utilized for detecting the NO_3^- sources (Mayer et al., 2002). As the NO_3^- origin is widely connected to the entire N cycle, the $\delta^{15}N$-NO_3^- can be biased due to: i) chemical, physical, and biological transformations of materials within the soil or groundwater that produce or remove the nitrogen compounds; ii) mixing of several distinct NO_3^- sources; and, iii) kinetic isotopic fractionation (Kellman and Hillaire-Marcel, 1998). As such, the $\delta^{15}N$ signature alone is not enough for robust and decisive identification of NO_3^- sources. Therefore in recent years, dual isotope approaches (combination of $\delta^{15}N$ and $\delta^{18}O$) have been widely utilized and expected to provide more conclusive information for detecting NO_3^- sources (Aravena and Robertson, 1998; Seiler et al., 2005).

1.2.5. $\delta^{15}N$ and $\delta^{18}O$ of NO_3^- Sources

$\delta^{15}N$-NO_3^- has been used for source discriminations since the early 1970s. The first study to utilize $\delta^{15}N$-NO_3^- and was reported in Kohl et al. (1971) for evaluating the significance of fertilizer contribution in the Sangamon River, Illinois. Several studies reported the representative $\delta^{15}N$ values for various nitrogen sources based on distinct $\delta^{15}N$ values. In nature, terrestrial materials have $\delta^{15}N$ composition between -20 and 30‰. The dominant source of nitrogen is the atmosphere with $\delta^{15}N$ value of 0‰. Synthetic inorganic fertilizer and animal waste have distinctive $\delta^{15}N$-NO_3^- values. Synthetic fertilizer produced by the fixation of atmospheric N_2 have $\delta^{15}N$-NO_3^- values in the range of -6 to +6‰ that are uniformly lower than the other sources (Xue et al, 2009). $\delta^{15}N$-NO_3^- values of animal waste are generally enriched in $\delta^{15}N$ (+10 to +25‰; Kreitler, 1979) relative to other nitrogen sources mainly because of: i) volatilization $\delta^{15}N$-depleted NH_3 during storage, treatment and application of animal waste; and ii) subsequent oxidation of NH_3 to microbial NO_3^- with enriched $\delta^{15}N$ (Kendall, 1998; Xue et al, 2009). Isotopic compositions of atmospheric and soil NO_3^- are not distinctive and overlap with that of fertilizer and animal waste.

The $\delta^{18}O$-NO_3^- values also have been used to determine NO_3^- sources (Mayer et al., 2002; Pardo et al., 2004). The wide range of $\delta^{18}O$-NO_3^- values (-10 to +21‰) in source materials indicates multiple reasons which include: i) fractionation of $\delta^{18}O$ from its source compositions (O_2 and H_2O) during atmospheric processes (evaporation); ii) significant isotope fractionation during the incorporation of oxygen from H_2O and O_2 into the newly formed microbial NO_3^- etc. Amberger and Schmidt (1987) analyzed several types of anthropogenic NO_3^- and determined that synthetic NO_3^- formed from atmospheric oxygen has a distinctive $\delta^{18}O$ value (+18 to +22‰). All three oxygens in synthetic NO_3^- are derived from atmospheric O_2 (+23‰) and hence the $\delta^{18}O$ values are similar to that of O_2. Wassenaar, 1995 demonstrated $\delta^{18}O$ as a more useful tool than $\delta^{15}N$ to separate atmospheric NO_3^- from microbial NO_3^- due to its marked contrast in isotopic signatures. The $\delta^{18}O$-microbial NO_3^- are thought to be derived from atmospheric $O_2 \approx$ +23‰ (Kroopnick and Craig, 1972) and environmental H_2O (-30 to +5‰) with 1:2 ratio.

1.2.6. Redox Process

Oxyanions (nitrate, selenate/selenite, and sulfate) are common constituents in the coal mining environment. A common feature of these three oxyanions is that their primary occurrences are largely dependent on redox conditions of the system. Change in redox condition can alter their oxidation states and can remove them from the aqueous system. The removal or reduction processes of these oxyanions occur systematically based on their free energy yield: NO_3^-, SeO_4^{2-}, and SO_4^{2-} (Figure 2). In the presence of dissolved oxygen, microorganisms will use O_2 as a terminal electron acceptor since it is the most energetically favorable oxidant for the reaction to proceed and provides the greatest free energy. In the absence of oxygen, oxyanions will be used as terminal electron acceptors in order of their free energy. Any microbial reduction process (e.g., denitrification) largely depends on the following factors: i) the absence or low levels of oxygen; ii) the presence of specific microbes; and iii) a labile electron donor, usually in the form of dissolved organic carbon (Postma et al., 1991; Cornwell et al., 1999). In the absence of organic carbon, other substances such as pyrite can be used as the electron donors (Postma et al., 1991; Korom et al., 2005; Korom et al., 2012).

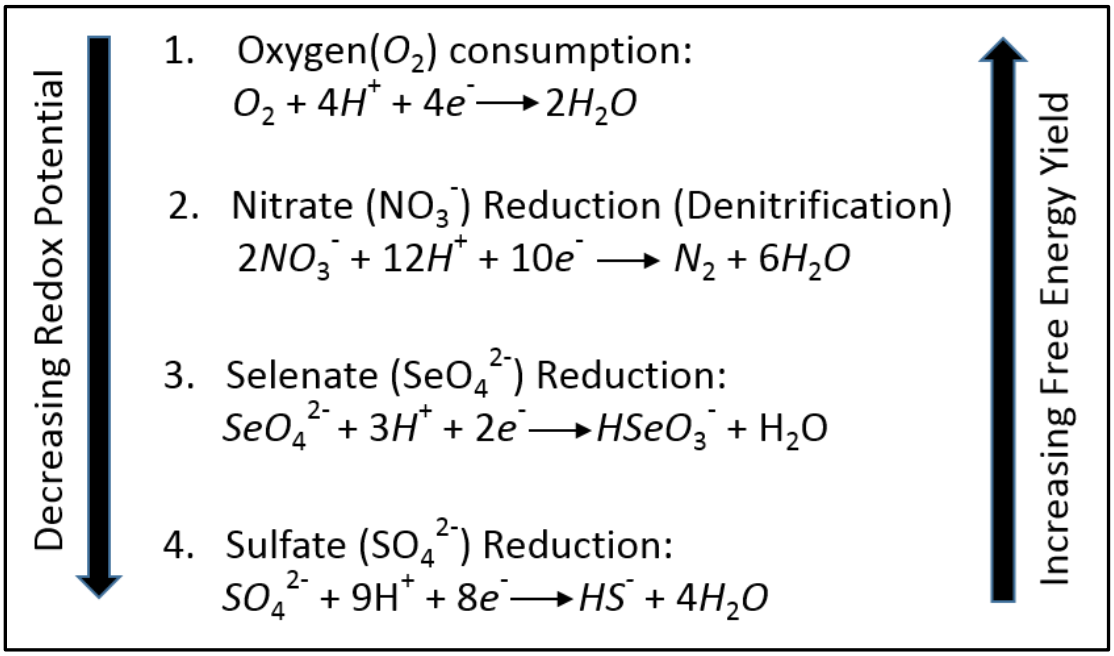

Figure 2. The sequence of redox process in order of decreasing redox potential and increasing free energy yield (modified after Stumm and Morgan, 1996).

1.2.7. Nitrification

Nitrification is one of the most important processes in the nitrogen cycle that governs the fate of nitrogen from explosives in an oxic environment. It is a multi-step biological oxidation process of NH_4^+ or NH_3 facilitated by autotrophic organisms (Focht and Verstraete, 1977; Killham, 1986), and produces microbial NO_3^- as the end member. During the nitrification process, NH_4^+ or NH_3 is oxidized to NO_2^- followed by oxidation of to NO_3^-, mediated by a different sets microorganisms. Nitrification can be presented by the following equations:

$NH_4^+ + OH^- \rightarrow NH_3 + H_2O$ …….. (4)

$NH_3 + O_2 + 2H^+ \rightarrow NH_2OH + H_2O$ ……..….. (5)

$NH_2OH + H_2O \rightarrow NO_2^- + 5H^+$ ……..…….. (6)

$2NO_2^- + O_2 \rightarrow 2NO_3^-$ ……..……....… (7)

Microbial NO_3^- can have a wide range of $\delta^{18}O$ values depending on the ammonium pool, background $\delta^{18}O$ values of NH_4^+, O_2, and H_2O and fractionation factors (Kendall, 1998; Clark and Fritz, 1997). During nitrification ($NH_4^+ \rightarrow NO_3^-$) three oxygen atoms are incorporated into the newly formed NO_3^- molecule, two of which are derived from water (Hollocher, 1984; Yoshinari and Wahlen, 1985), and the third one is from atmospheric O_2. Multiple experiments to determine the $\delta^{18}O$-NO_3^- derived from nitrification in water and unsaturated soils have reported quite contrasting results. Based on soil incubation experiments, Amberger (1987) suggested that NO_3^- produced by nitrification could have negative $\delta^{18}O$ values. Voerkelius and Schmidt (1990) published data on $\delta^{18}O$-NO_3^- of 0 ± 2‰ generated in soil column experiments. In recent years, multiple laboratory soil incubation studies reported $\delta^{18}O$ values of between +2 and +17‰ as typical for NO_3^- derived from the nitrification (Kendall, 1998).

1.2.8. Denitrification

Denitrification is a multi-step, natural, irreversible geochemical process that produces various nitrogen oxides as intermediate products and results in the chemical or biologically mediated reduction of NO_3^- to N_2. Denitrification occurs under anoxic conditions when the dissolved O_2 concentration is less than 0.5 mg/L and NO_3^- becomes the major oxygen source for

microbes. Heterotrophic denitrification happens when microbes use organic carbon (methanol, ethanol etc.) as an electron donor, and break apart NO_3^- to gain O_2 resulting in the reduction of NO_3^- to nitrous oxide (N_2O), and finally nitrogen gas (N_2). Equations for heterotrophic denitrification using different organic carbon sources are given below:

$6NO_3^- + 5CH_3OH \rightarrow 3N_2 + 5CO_2 + 7H_2O + 6OH^-$ ……...….... (8)

$4NO_3^- + 3CH_4 \rightarrow 2N_2 + 3CO_2 + 6H_2O$ …….. (9)

$2NO_3^- + 3CH_2O \rightarrow N_2 + 3CO_2 + 3H_2O$ ……..……...… (10)

Autotrophic denitrification uses autotrophic denitrifiers for which energy source is derived from inorganic oxidation-reduction reactions of elements such as pyrite as an electron donor to reduce NO_3^- to N_2. The equation for autotrophic denitrification using pyrite is given below:

$3FeS_2 + 8NO_3^- \rightarrow 4N_2 + 6SO_4^{2-} + 3Fe^{2+}$ ……..… (11)

Microbial denitrification is an important process that leads to significant alteration of the isotopic composition of NO_3^-. Depending on the redox condition and availability of organic carbon as an electron donor, microbes use NO_3^- as an electron acceptor. The effects of kinetic isotope fractionation during microbial denitrification are responsible for preferential transferring of the lighter isotope (i.e., ^{14}N) to N_2. As a result, an enrichment of the heavy isotopes (^{15}N and ^{18}O) is observed in the remaining NO_3^- (Mariotti et al., 1981; Mayer et al., 2002; Fukada et al., 2003). Nitrogen and oxygen isotope enrichment factors of denitrification are between -40‰ and -5‰ (Smith et al., 1991; Sebilo et al., 2003), and -18‰ and -8‰ (Fukada et al., 2003; Lehmann et al., 2003), respectively. Some studies reported that there is a linear relationship between the enrichment of ^{15}N-NO_3^- and ^{18}O-NO_3^- by a factor of 1.3:1 to 2:1. (Aravena and Robertson, 1998; Fukada et al., 2003).

1.2.9. NO_3^- as an Inhibitor of Selenium Reduction

Thermodynamic calculations support NO_3^- reduction first at a higher redox potential than selenate (Figure 2) and therefore NO_3^- reduction is theoretically favored at higher energy yield. Multiple laboratory and field studies were conducted to examine the inhibition of selenate reduction by the presence of NO_3^-. Zhao et al. (2014) reported that complete removal of NO_3^- is

essential for significant selenate reduction to occur. This finding supports an earlier finding that demonstrated the inhibition of selenate reduction by the NO_3^- (Oremland et al., 1989; Weres et al., 1990; Bailey et al., 2012, White et al., 1991). Some studies have also examined the potential of simultaneous reduction of NO_3^- and selenate in the presence of NO_3^- as high as 8 mg/L (Oremland et al., 1991). However a threshold concentration of NO_3^- at which NO_3^- and selenate reduction can occur simultaneously is yet to be defined since it is influenced by the NO_3:Se concentration ratio between different environments (Oremland et al., 1990).

1.2.10. NO_3^- Flushing

Although studies addressing nitrate flushing through the unsaturated waste rock dumps are scarce in the literature, several researchers have described the water flow through the unsaturated zone of the waste rock dump using conservative tracers at scales ranging from laboratory to the field (e.g., Eriksson et al., 1997; Nichol et al., 2005; Amos et al., 2015). Amos et al. (2015) reported the presence of two major flow pathways: matrix and preferential flow. The dominance of each flowpath while transporting solutes through the waste rock dump actively depends on waste rock properties such as particle size distribution, compaction, and the hydrological conditions governed by the magnitude and duration of precipitation, and infiltration of snowmelt and rain events (e.g., Smith and Beckie, 2003; Nichol et al., 2005). Nichol et al. (2005) suggested the influence of a preferential flow in response to large rainfall events using a chloride-tracer experiment, while Neuner et al. (2013) concluded the dominance of matrix flow in Diavik test piles even in response to a large rain event. The controls of flow pathways also varied with scale in a way that Eriksson et al. (1997) reported matrix flow at the laboratory scale, and the dominance of preferential flow at the field scale. Such results also question the applicability of the small scale results to larger field scale. Recently, Appels et al. (2016) improved our understanding of the impacts of texture, complex structures, and moisture content on leaching efficiency using a physically based 2D numerical experiment. Appels et al. (2016) further emphasized the utility of their findings on future dump design.

1.3. Thesis Outline

In the following sections, this thesis describes the materials and methods, results, discussions, summary and conclusions and recommendations.

Section 2 describes the materials and methodology applied to meet the objectives discussed in section 1.1. This study heavily relied on solid samples collected from a drilling program performed by Teck. Continuous core and cutting samples were obtained from a series of boreholes drilled using sonic and air rotary methods. This study involved multiple datasets of NO_3^- from pre-blast, fresh-blast, waste rock dump ranging in depositional age from 1982 to 2012 and WLC rock drain to define the source, distribution, and fate of NO_3^- in the dump. Dual isotope analyses on NO_3^- were performed to delineate the source of NO_3^- as well as to understand the evolution of geochemical control (nitrification/denitrification) that can affect the fate of NO_3^- in the waste rock dump. This study also used NO_3^- data from humidity cells (HCs) and leach pads (LPs), collected on behalf of Teck by SRK Consultants, to characterize the flushing mechanism of NO_3^- at the smaller scales and compare the findings with field scale dump.

Section 3 reports the statistical summaries of pre-blast, fresh (fresh-blast, HCs and LPs) and aged waste rock samples in conjunction with isotope ratio measurements on NH_4NO_3 prill ($\delta^{15}N\text{-}NH_4^+$, $\delta^{15}N$- and $\delta^{18}O\text{-}NO_3^-$), pre-blast ($\delta^{15}N$-TN), fresh-blast ($\delta^{15}N$- and $\delta^{18}O\text{-}NO_3^-$), aged waste rock and rock drain samples ($\delta^{15}N$- and $\delta^{18}O\text{-}NO_3^-$). This section also reports estimation of leaching efficiency (E_L) using NO_3^- and flow data from HC and LP experiments at the smaller scales and high-resolution WLC boreholes samples at the field scale, respectively.

Section 4 provides a comprehensive discussion on the findings reported in section 3. The results of this study are compared with previous scientific studies and findings to provide uniqueness and novelty of the current study. Section 5 provides a summary and conclusions inferred from this study. Finally, Section 6 states the recommendations for future study based on the limitations of the current study.

2. MATERIALS AND METHODS

2.1. Sampling of Waste Rock

A drilling program was carried out at the LCO West Line Creek (WLC) dump to collect waste rock samples for analyses. Drilling and sampling were conducted using a truck-mounted sonic drill rig (Sonic Rig 1524), and a truck-mounted air rotary drill rig (Foremost DR 24 drill) between July and September 2012. The LCO-WLC dump is not vegetated nor fertilized. It is approximately 3.5 km long, up to 1 km wide, and covers a surface area of about 2.7 km^2 with an average thickness of 100 m (AMEC Environmental & Infrastructure, 2013) (Figure 1c). Samples collected were deposited between 1982 and 2012 (i.e., 1982-1990, 1991-1994, 1994-1998, and 2009-2012) (Hendry et al., 2015).

Four vertical sonic boreholes were drilled in the dump to a maximum depth of 87 m below ground (BG) surface (Table 1). Two boreholes (LCO-WLC-12-02a and 12-02b) were drilled in the northern portion, and two (LCO-WLC-12-05a and 12-05b) in the southern portion of the dump (Figure 1c). Sonic boreholes were drilled using a 0.10 m internal diameter (ID) and occasionally 0.15 m ID x 3.05 m long core barrel. Core recovery was approximately 90%. After recovery from the core barrel, each sonic core was transferred into a plastic sleeve. The two ends of each sleeve were immediately tied and placed in a 0.1 m diameter PVC half pipe. The cores were then moved to the onsite core shed where the sleeves were cut open. Prior to sample collection, the outer 1-5 mm of core was removed to reduce any potential cross-contamination during drilling. Approximately 2-3 kg of each core was collected for chemical analyses at a sampling interval of approximately 1 m. Samples were placed in medium sized Ziploc® bags (180 mm x 190 mm) and atmospheric air squeezed out. These bags were then placed into large Ziploc® bags (270 mm x 270 mm) and the atmospheric air squeezed out before sealing. The double bagged cores were kept at about 4° C during transportation from the field to the UofS Satellite Lab at Hillcrest Mines, Alberta. Subsequently, all bagged samples were vacuum sealed in Food Saver bags (200 mm x 270mm), stored in coolers and shipped to the Environmental Geochemistry Laboratory (AEG), University of Saskatchewan (UofS) for processing.

Two air rotary holes (LCO-WLC-12-05C_1 and -12-05C_2) were drilled to about 181 m BG in the southern part of the dump (Table 1; Figure 1c). Cutting samples were collected at about 3 m depth intervals. Immediately after retrieval, approximately 500 g of samples were placed in

medium sized Ziploc® bags and followed the procedure of sample handling and processing as described for sonic core samples, above.

Grab samples (2-4 kg) of waste rock were collected between February and August 2012 during placement of the Turn Creek dump at FRO (FRO-TCR). Samples were collected from haul truck loads during the placement of bottom, mid, and upper portions of the dump. Before the sample collection, an excavator or loader was used to sift waste rock through a 100 mm grizzly screen to obtain samples with a diameter less than 100 mm. These samples were collected within 10 d of blasting to represent fresh-blast rock. Pre-blast Mist Mountain Formation rock samples were collected from diamond drilled corehole MM1306 at LCO. The corehole was drilled in January 2014 and samples collected between 3 and 360 m depth BG on February 2014. Sample handling and processing of the fresh and pre-blast samples were as described for sonic core samples, above.

2.2. Porewater Sampling, Water Extractions and Chemical Analyses

A high-pressure mechanical squeezer was used to squeeze porewater from sonic core samples from 12-02a (n=5), 12-05a (n=17), and 12-05b (n=12). Core samples (100-300 g) were broken up and packed in the cylinder of the squeezer. A piston was then inserted in the cylinder and a pressure of about 50 MPa applied for 3-5 d (Hendry et al., 2013). Dissolved porewater samples were expelled through a 0.45 μm stainless steel filter at the base of the cylinder into a clean syringe. The volumes of porewater ranged from 0-14 cm^3, depending on the water content of the samples. After no additional water could be squeezed from the core samples, the water samples were split into a series of bottles for specific analyses. Before the porewater was separated, pH was measured using an Oakton 110 Series. The pH of dissolved porewater ranged from 7.75 to 8.64 and the average was 8.01. In this study, only NO_3^-- and NO_2^--N analyses from squeezed samples (n=34) were considered. Leached porewater ionic concentrations (mg/L) from the sonic (12-02a, n=56; 12-02b, n=29; 12-05a, n=12), air rotary (12-05C_1, n=51; 12-05C_2, n=57), diamond drill (MM1306 pre-blast samples, n=22), and fresh-blast samples from TCR (n=36) were determined using the aqueous leached method (MEND, 2009). All samples were oven-dried, disaggregated and crushed with a ceramic mortar and pestle, then placed in 1 L high density polypropylene bottles (HDPE) with Milli-Q water at a 3:1 water to solids ratio, and agitated using a shake table for 48 h.

Table 1: Location and number of solid and rock drain water samples analyzed.

BOREHOLE ID	OPERATION	BOREHOLE DEPTH (m)	SQUEEZED POREWATER	WATER EXTRACTION	CHEMICAL ANALYSES	$\delta^{15}N\text{-}NO_3^-$ & $\delta^{18}O\text{-}NO_3^-$
Sonic drill holes						
LCO-WLC-12-02a	Line Creek	87	5	56	61	14
LCO-WLC-12-02b	Line Creek	20	0	29	29	9
LCO-WLC-12-05a	Line Creek	66	17	12	29	3
LCO-WLC-12-05b	Line Creek	59	12	0	12	0
Rotary drill holes						
LCO-WLC-12-05C_1	Line Creek	163	0	51	51	0
LCO-WLC-12-05C_2	Line Creek	181	0	57	57	7
Grab samples						
FRO-TCR Fresh-Blast Rock	Fording River		5	36	41	4
Pre-blast diamond drill hole						
MM1306	Line Creek	360	0	22	22	0
Rock Drain Water Samples						
WLC CULVERT	Line creek				477	12

After allowing the solids to settle for 24 h, subsamples of water were decanted into 50 mL HDPE centrifuge vials and centrifuged at 3000 rpm until clear. The supernatant samples were filtered with PES 0.45 µm filters and collected in 30 mL HDPE bottles for cations, anions, trace elements, $\delta^{18}O$- and $\delta^{15}N$-NO_3^-.

Dissolved and leached porewater samples were stored at 4º C prior to chemical analyses. The NO_3^-- and NO_2^--N concentrations were measured using a Dionex ICS2100 coupled to a Dionex AS-AP Autosampler with Dionex IonPac AS9-HC 2×2 mm exchange. The analysis performed was consistent with the methods described in EPA Method 300.1 (Hautman and Munch, 1997). Method detection limits (MDL) for NO_3^-- and NO_2^--N were 0.03 and 0.05 mg/L, respectively. Analytical accuracy and precision were <5% for both analytes.

The water extractable NO_3^--N concentration (C; mg/kg) was calculated by multiplying the leached porewater NO_3^--N concentration of the extract (C_e; mg/L) by the ratio of mass of water used in the aqueous extract (Ww) to the dry mass of sample (Ws) used for the chemical extraction.

$$C = C_e * \frac{Ww}{Ws} \quad \text{..... (12)}$$

The porewater equivalent NO_3^--N concentration (C_{pw}; mg/L) was estimated by multiplying the leached porewater NO_3^--N concentration of the extract (C_e; mg/L) by the ratio of gravimetric water content (GWC) of the extraction samples (ω_e) to that of the original sample (ω_s) as described by the following equation:

$$C_{pw} = C_e * (\frac{\omega e}{\omega s}) \quad \text{..... (13)}$$

Values of ω_s were measured for the sonic core samples based on the method described in ASTM D2216-10 (2010) and reported by Barbour et al. (2016). The *in situ* GWC of the air rotary samples was assumed to be that of the values measured on sonic core samples from associated depths and location. For air rotary samples collected from depths greater than the sonic samples, the mean ω_s from the sonic samples was used to estimate the water content of the air rotary samples.

Quartile-quartile plots, Pearson's chi squared (χ^2, Plackett, 1983) and F (Box, 1953) tests were conducted on NO_3^--N concentration data from WLC boreholes and pre-blast rock samples. Quartile-quartile plots showed the NO_3^--N concentration data deviated from the normally distributed dataset while the logarithm of concentration data [$\log_{10}$ (conc.)] were consistent with the normally distributed dataset. Pearson's chi-squared tests showed that the calculated test statistics did not exceed the critical values of $\chi^2_{0.95}$ at a level of significance α=0.05 and, because the test statistics did not exceed the critical values, the null hypothesis (Ho=the NO_3^--N datasets are normally distributed) could not be rejected with the selected level of significance. This was confirmed by the F test results that showed the calculated F statistics did not exceed the critical values of $F_{0.95}$ at a level of significance α=0.05. Based on both chi-squared and F tests, it was concluded that $\log_{10}$ (conc.) datasets were log normal. Student's t tests were conducted on $\log_{10}$ (conc.) at a confidence interval of 95% to assess statistically significant differences in NO_3^--N concentrations of water extractable waste rock samples from different boreholes.

2.3. Humidity Cell and Leach Pad Experiments

Laboratory humidity cell (HC) and field-scale leach pad (LP) experiments were conducted using waste rock from LCO. Three different types of waste rock materials were tested: Type-1 was comprised of interburden containing mudstones and traces of coal; Type-2 was sandstone containing mudstone and coal; and Type-3 was siltstone containing a mixture of siltstone, mudstone, coal, and sandstone. X-ray diffraction spectra indicated that quartz, kaolinite, illite-muscovite and carbonate, including dolomite and siderite, are the dominant minerals in the samples and pyrite was the most common sulfide minerals in the waste rock.

The HCs were constructed from 0.1 m dia x 0.2 m long plexiglass pipes. Solid plexiglass base plates with leachate drainage holes were attached to the base of each cell. A perforated plexiglass plate was installed inside the pipes approximately 25 mm above the base plates to support the weight of the samples, and allow the upward flow of air through the bottom of the cell and downward flow of leachate. The plates were covered with screen cloth to prevent the loss of fine-grained sediments. Tests were carried out using 1 kg of air-dried waste rock placed loosely into the plexiglass pipe, filling approximately 75% of the available volume. Nine HC tests (two tests for each type, two laboratory duplicates from type-1 and 2, and one method blank) were initiated in May 2009. Testing was conducted in three stages over 7 d cycles. The

stages consisted of 3 d of aeration with dry air followed by 3 d of aeration with humidified air (over and through the samples) and followed by flushing of the sample with 0.5 L of deionized (DI) water on day 7 (MEND, 2009). Leachate was collected at two-week intervals for the first 15 weeks. After week 15, the frequency of sampling was reduced to monthly and after week 195, sampling frequency was reduced to once every four months. Testing was reduced to five HC tests (one from each type, a duplicate from type-1 and the method blank) in May 2010 (week 51) because of the good reproducibility between duplicates. The experiments were terminated in December 2013 (week 235). Effluent samples were analyzed for NO_3^-- and NH_3-N, and other anions and cations, and trace elements by two commercial laboratories, Maxxam and Cantest. The reported MDL of NO_3^-- and NH_3-N were 0.002 and 0.005 mg/L; and 0.02 and 0.01 mg/L for Maxxam and Cantest, respectively.

The LPs were constructed between October 15 and November 5, 2008 at the North Line, LCO. Stages of leach pad construction were: base construction, liner and drainage pipe installation, and loading the leach pads with waste rock. Base construction started with the placement of 0.05 m minus crushed rock to create a base area which was 20 m long and 12 m wide. The bases were then compacted using a smooth drum vibratory compactor and shaped with a Linkbelt 240 LX excavator to make a central drainage trench at a gradient of 2-5% along the short axis of the pad which provided ample drainage toward the trench (SRK, 2010). A containment berm of crushed rock was then constructed around the sides of the base area. The base area was covered with a layer of protective geotextile overlain by a 4-mm thick bituminous impermeable geomembrane. The drainage collection system consisted of 4-m long sections of 0.1 m diameter PVC pipes placed along the central drainage trench. The pipes were wrapped in filter cloth to minimize clogging with fines. Drainage gravel (5 cm minus crushed rock) was placed around and on top of the drainage pipes to fill the central drainage trench to the level of the leach pad base and geotextile placed on top of the gravel to enhance filtering capacity.

The three waste rock types were then placed within the prepared leach pads. The volume of rock placed in each LP ranged from 125 to 250 m^3 (based on length and width measurements) and the mass of waste rock estimated to range from 213 to 425 tonnes. This estimate was made assuming the LCM (loose cubic meter) density of the rock was 1.7 T/m^3. The final geometry of the LPs was a truncated pyramid of waste rock approximately 2.5 m high with 2:1 side slopes.

Each LP was instrumented to monitor infiltration, temperature, pore gas composition, and volumetric water content (VWC) at four depth intervals (0.1, 0.5, 1.0 and 1.5 m below the top of LPs). Tipping bucket flow gauges were installed at the outlet of each drainage pipe to measure water fluxes from each LP on a monthly basis. Drainage water samples were collected monthly and analyzed for NO_3^--, NO_2^-- and NH_3-N and other anions, cations, and trace elements by commercial laboratories. The reported MDL for NO_3^--, NO_2^-- and NH_3-N were 0.005, 0.001 and 0.005 mg/L, respectively.

2.4. Nitrogen species in the WLC Rock Drain

Rock drains, such as the one existing at the base of the LCO-WLC dump along the pre-disturbance West Line Creek (Figure 1c), are formed by segregation of the waste rock during dumping as the largest particles (boulders) move to the base of the slope creating a basal rubble zone (Morin et al., 1991). The rock drain collects water draining vertically through the dump and combines it with water flowing from the natural watershed. Water released from the downstream end of the rock drain is conducted along both a surface creek and a constructed underground culvert to a monitoring point ~270 m downstream (WRD on Fig 1c). Drainage from the WLC rock drain began shortly after the beginning of dump construction (in 1982). From January 1999 to November 2009, discharge measurements were estimated based on a relationship between discharge at the rock drain and the nearby Line Creek flow gauging station (Government of Canada Water Office Station 08NK022) which is located 5.5 km southwest of the WLC rock drain sampling site. Beginning in November 2009, daily discharge measurements at the outlet were obtained from an instream bubbler installed beside a weir. Daily flow data from the rock drain and Line Creek were used to obtain a linear regression for data from November 2009 to December 2012 (r^2=0.8). Likewise, a linear regression for 2010 only (r^2=0.9), a lower flow year, and 2012 only (r^2=0.92), a higher flow year, were also obtained. This allowed the pre-2009 flow data to be estimated based on the magnitude of yearly flow at Line Creek. If the maximum flow rate at Line Creek during the estimated year was below 13 m^3/s, the 2010 regression was used, and if the maximum flow was above 13 m^3/s, the 2012 regression was used.

Monthly rock drain samples were collected from 2000 to 2010. Post-2010, samples for NO_3^- analysis were collected on a weekly basis (March-August) and a monthly basis (September-February) till 2014. A commercial laboratory measured NO_2^-- and NO_3^--N

concentrations. Additional water samples were collected daily (July-August 2012), weekly (September-October 2012 and May-August/September 2013-2014), and monthly (October-April 2013-2014) and analyzed for NO_2^-- and NO_3^--N using the methods described above for squeezed porewaters. Samples were field filtered, refrigerated, and shipped to AEG for processing and analysis of NO_2^-- and NO_3^--N. The reported MDLs for NO_2^-- and NO_3^--N were 0.05 and 0.03 mg/L, respectively.

The rock drain flow and solute concentration data were used to calculate yearly estimates of discharge and solute load from the WLC dump to the rock drain. Given the available chemistry, data was intermittent, while post-2009 flow data was nearly continuous, concentrations were averaged in between sampling periods and daily estimates of load calculated. Pre-2009 flow rates at each sampling time were estimated using the relationship to Line Creek flow and the load calculated based on the average flow and concentration between sampling periods.

2.5. O_2 Gas Concentrations

Multi-level Continuous Multi-channel Tubing (CMT) Waterloo gas monitoring ports were installed at 12-02a (n=24 ports; 2-85 m BG) and 12-05C_2 (n=24 ports; 3-180 m BG) to measure pore gas concentrations with depth through the dump between August 2012 and April 2015. Four CMT's were also installed through the waste rock in each LP (0.1-1.5 m BG) between June, 2010 and October, 2013. Pore gas O_2 concentrations were measured using RKI Instruments Eagle® portable gas meter. The gas meter was calibrated with standards of known concentration of O_2 prior to each day of use. The accuracy of the meter was ±0.5% O_2. Prior to measuring the O_2 concentrations, one volume of standing gas was purged from the tubing using the Eagle® internal pump.

2.6. Isotope Analyses of N Species

The $\delta^{15}N$ of the total N on pre-blast solid samples (n=10) were analyzed using Continuous Flow-Elemental Analysis-Isotope Ratio Mass Spectrometry, with an analytical accuracy and precision of ±0.2‰ (Preston et al., 1983; Werner et al., 2001). The $\delta^{15}N$-NH_4^+ of the NH_4NO_3 blasting prills (n=2) was measured using the ammonium diffusion method with an

analytical accuracy and precision of ±0.2‰ (Sebilo et al., 2004). The $\delta^{15}N$ and $\delta^{18}O$ of soluble NO_3^- in NH_4NO_3 blasting prills (dissolving 10 mg of NH_4NO_3 prills in 100 mL DI water), leached porewater samples from FRO-TCR fresh-blast rocks (n=4), LCO-WLC waste rock dump (n=33) and rock drain samples (n=12) collected between June 2012 and September 2013 were analyzed using the denitrifier method (Casciotti et al., 2002; Sigman et al., 2001). Analytical accuracy and precision of these $\delta^{15}N$- and $\delta^{18}O$-NO_3^- analyses were ±0.3‰ and 0.7‰, respectively (Bohlke et al., 2003; Silva et al., 2000). All isotope analyses were performed at the Isotope Science Laboratory, Geoscience Department, University of Calgary, Canada. $\delta^{15}N$ and $\delta^{18}O$ values were referenced against three international standards (IAEA-NO_3^-, IAEA-N1 and IAEA-N2) and SMOW (Standard Mean Ocean Water), respectively and reported as per mil (‰).

3. RESULTS

3.1. Water Extractable and Porewater N Concentrations in Waste Rock

Statistical summaries and box and whisker plot of water extractable NO_3^--N concentrations in pre- (n=22) and fresh-blast rock samples (n=36) are presented in Table 2 and Figure 3, respectively. Pre-blast samples exhibited high frequency of samples having NO_3^--N concentrations ranging from 0.20-0.30 mg/kg. The maximum and mean NO_3^--N concentrations for these samples were 0.37 and 0.20±0.10 mg/kg, respectively and 18% of the NO_3^--N concentrations were below the MDL. In contrast to pre-blast samples, NO_3^--N concentrations in fresh-blast samples were variable (below MDL to 241 mg/kg; Table 2) exhibiting a positively skewed Gaussian distribution (i.e., mean values are greater than median values) with median and mean NO_3^--N concentrations of 12.6 and 27.6±47.4 mg/kg, respectively. About 83% of the NO_3^--N concentrations in the fresh-blast samples were greater than the mean concentration in the pre-blast samples while 17% of samples were below MDL. In contrast to the NO_3^--N concentrations, all NO_2^--N concentrations from both pre- and fresh-blast samples were below MDL (Table 4). Statistical summaries and box and whisker plot of water extractable NO_3^--N concentrations of waste rock samples from both boreholes are presented in Table 2 and Figure 3, respectively. NO_3^--N concentrations with depth are presented in Figure 4. In keeping with the fresh-blast samples, NO_3^--N concentrations from dump samples (including individual borehole data sets) exhibited slightly positive skewed Gaussian distributions and were variable; the overall sample-to-sample variability at the scale of the NO_3^--N measurements was high with minimum and maximum measured NO_3^--N concentrations in the dump of below MDL and 24.5 mg/kg, respectively (median= 1.26 mg/kg, mean=2.43±3.81 mg/kg; Table 2). NO_2^--N values for all samples (except one) were below MDL (Table 4). At borehole 12-02, NO_3^--N concentration <40 m BG surface ranged from below MDL to 24.5 mg/kg. The median and mean NO_3^--N concentration were 2.86 and 4.97±5.43 mg/kg. Whereas NO_3^--N concentration >40 m BG surface ranged from below MDL to 4.80 mg/kg. The median and mean NO_3^--N concentration were 0.38 and 0.83±1.15 mg/kg (Table 2).

Porewater equivalent NO_3^--N concentrations (mg/L) of fresh-blast and waste rock samples estimated from leached porewater NO_3^--N concentrations (mg/L), are presented in Table 2 and figure 3. NO_3^--N concentrations vs. depth in the dump are presented in Figure 5.

Table 2: Summary (descriptive) statistics of water extractable and porewater equivalent NO_3^--N concentrations.

Mine Site	n	Water extractable NO_3^--N (mg/kg)							Porewater equivalent NO_3^--N (mg/L)						
		Mean	Median	Max	Min	St Dev	Skew	Kurt	Mean	Median	Max	Min	St Dev	Skew	Kurt
LCO	205 (28)	2.43	1.26	24.5	<0.09	3.81	3.37	12.9	48.3	22.2	486	<1.56	78.9	3.48	13.9
LCO-WLC-12-02	85(4)	3.65	2.22	24.5	<0.09	4.92	2.62	6.87	79.6	48.1	486	<1.56	105	2.52	6.23
LCO-WLC-12-02a (<40 m BG)	58(1)	4.97	2.86	24.5	<0.09	5.43	2.22	4.29	109	65.6	486	<1.56	115	2.15	3.85
LCO-WLC-12-02a (>40 m BG)	27(3)	0.83	0.38	4.80	<0.09	1.15	2.32	5.23	15.8	7.31	91.5	<1.56	22.0	2.32	5.23
LCO-WLC-12-05	120(24)	1.56	0.71	16.4	<0.09	2.44	3.74	17.9	26.1	11.9	275	<1.56	40.7	3.74	17.9
FRO Fresh-blast	36(6)	27.6	12.6	241	<0.09	47.4	3.25	12.3	497	227	4343	<1.56	854	3.25	12.3
Pre-blast	22(4)	0.20	0.20	0.37	<0.09	0.10	0.03	0.9	N/A	N/A	N/A	N/A	N/A	N/A	N/A

Notes: Values in brackets represent the number of concentrations below the average calculated method detection limits (MDL) of 0.09 mg/kg and 1.56 mg/L for water extractable and porewater equivalent NO_3^--N concentrations, respectively. No NH_3 analyses were conducted.

Table 3: Summary (descriptive) statistics of dissolved porewater NO_3^--N concentrations.

Mine Site	n	Dissolved porewater NO_3^--N (mg/L)						
		Mean	Median	Max	Min	St Dev	Skew	Kurt
LCO	34 (2)	7.71	2.41	41.8	<0.03	10.6	1.89	3.44
LCO-WLC-12-02	5(0)	11.3	1.04	41.8	0.65	17.8	1.84	3.27
LCO-WLC-12-02a (<40 m BG)	N/A	N/A	N/A	N/A	N/A	N/A	N/A	N/A
LCO-WLC-12-02a (>40 m BG)	5(0)	11.3	1.04	41.8	0.65	17.8	1.84	3.27
LCO-WLC-12-05	29(2)	7.09	2.50	37.5	<0.03	9.24	1.78	3.31
FRO Fresh-blast	5(0)	473	394	1283	59.8	479	1.65	3.06
Pre-blast	N/A	N/A	N/A	N/A	N/A	N/A	N/A	N/A

Notes: Values in brackets represent the number of concentrations below the instrument method detection limit (MDL) of 0.03 mg/L for dissolved porewater NO_3^--N concentrations. No NH_3 analyses were conducted.

Table 4: Summary (descriptive) statistics of water extractable and porewater equivalent; and dissolved porewater NO_2^--N concentrations.

Mine Site	n	Water extractable NO_2^--N (mg/kg)		Porewater equivalent NO_2^--N (mg/L)		Dissolved porewater NO_2^--N (mg/L)	
		Max	Min	Max	Min	Max	Min
LCO	205(204) 34(33)	0.21	<0.15	3.56	<2.83	0.39	<0.05
LCO-WLC-12-02	85(85) 5(4)	<0.15	<0.15	<2.83	<2.83	0.39	<0.05
LCO-WLC-12-05	120(119) 29(29)	0.21	<0.15	3.56	<2.83	<0.05	<0.05
FRO Fresh-blast	36(36) 5(0)	<0.15	<0.15	<2.83	<2.83	3.39	0.29
Pre-blast	22(22)	<0.15	<0.15	N/A	N/A	N/A	N/A

Notes: Values in brackets represent the number of concentrations that were below average calculated method detection limits (MDL) of 0.15 mg/kg and 2.83 mg/L for water extractable and porewater equivalent, respectively and instrument method detection limit (MDL) of 0.05 mg/L for dissolved porewater NO_2^--N concentrations. No NH_3 analyses were conducted.

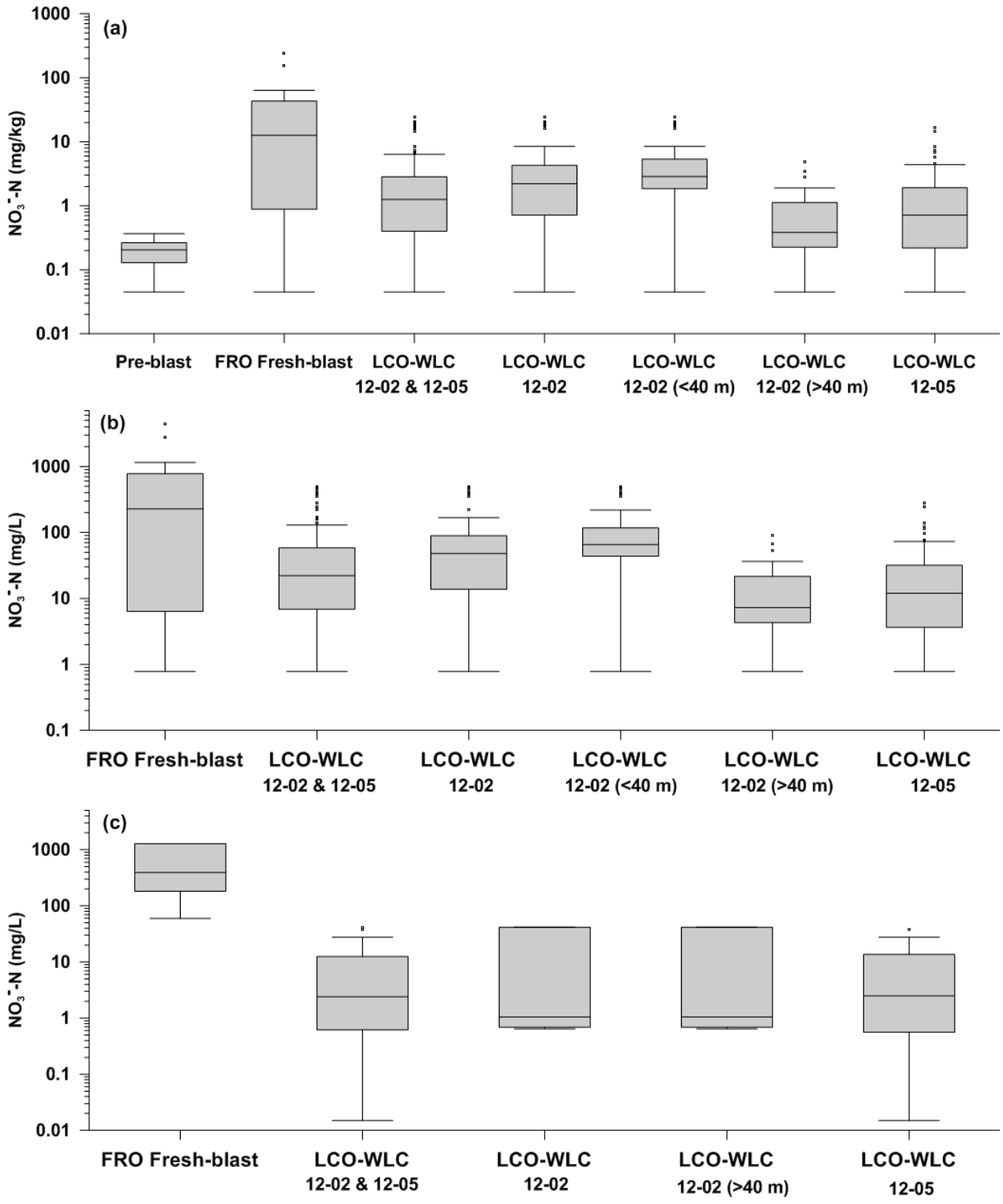

Figure 3. Box and Whisker plots of (a) water extractable, (b) porewater equivalent and (c) dissolved porewater NO_3^--N concentrations, respectively. The horizontal lines in the boxes are median, the lower and upper edges of the boxes are the 25th and 75th percentiles, respectively. The most extreme data points are considered as outliers and are plotted individually as solid black circles.

Median and mean NO_3^--N concentrations of fresh-blast and aged waste rock samples were 227 and 497±854 mg/L; and, 22.2 and 48.3±78.9 mg/L, respectively. The porewater equivalent NO_2^--N concentration of fresh-blast rock and all but one waste rock sample were below MDL (Table 4).

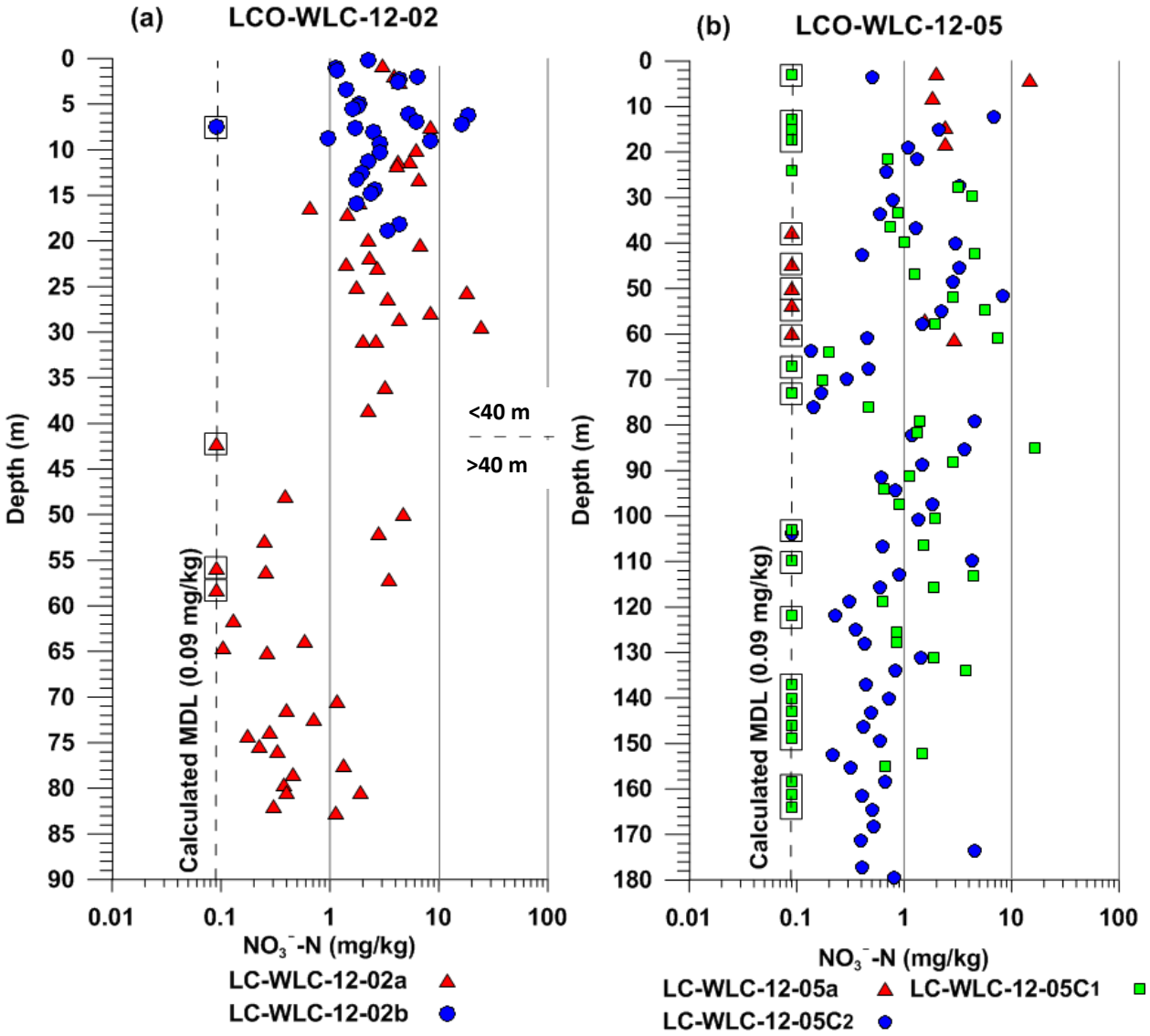

Figure 4. Water extractable NO_3^--N concentrations (mg/kg) of aqueous leached samples with depth in the waste rock dump at (a) LCO-WLC-12-02 (0-90 m BG in Y-axis) and (b) -12-05 (0-180 m BG in Y-axis) collected via sonic and air rotary drilling. Solid lines represent major grids for the x-axes. Vertical dashed lines represent calculated method detection limit (MDL; 0.09 mg/kg).

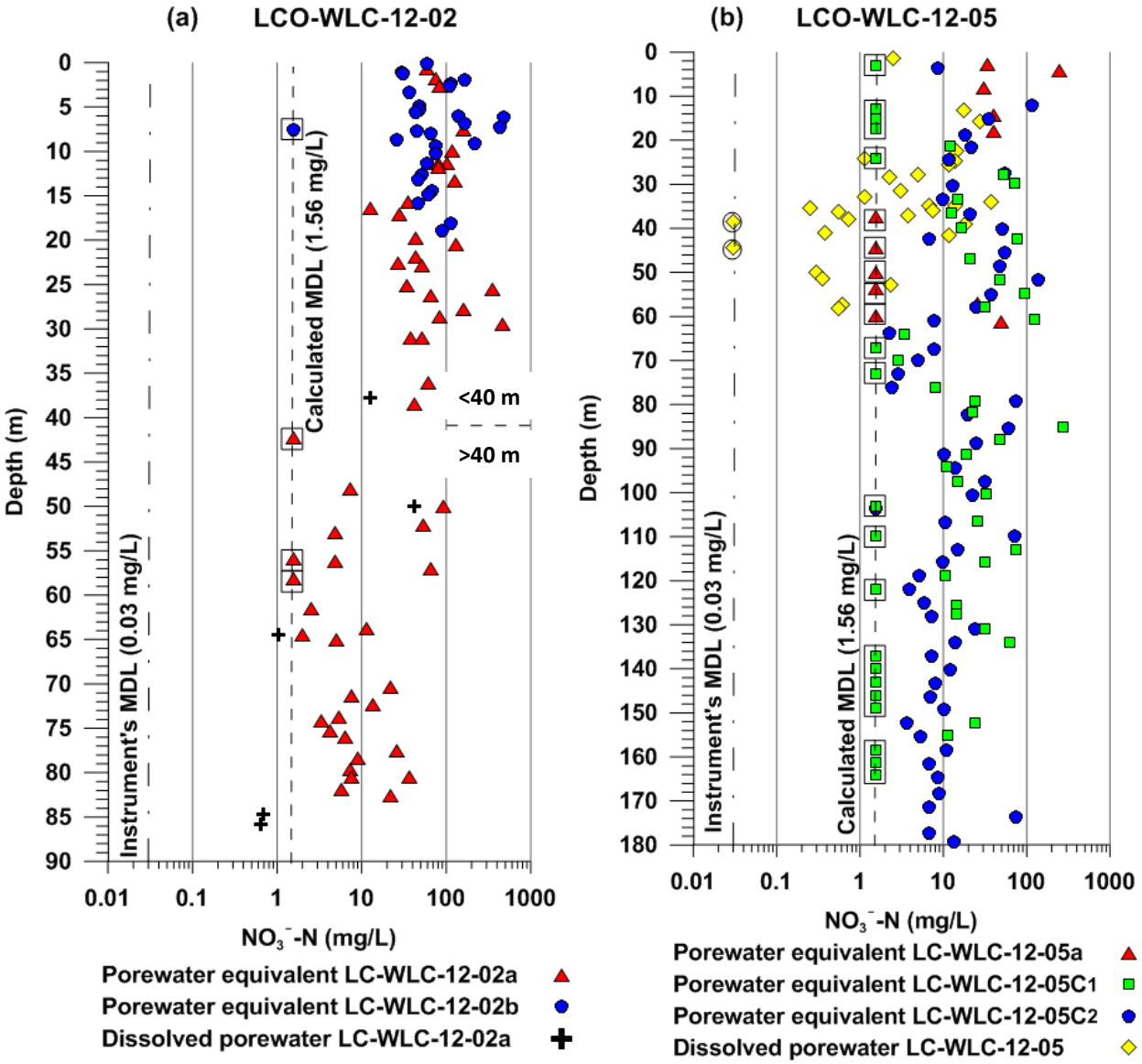

Figure 5. Porewater equivalent NO_3^--N concentrations (mg/L) of aqueous leached samples with depth in the waste rock dump at (a) LCO-WLC-12-02 (0-90 m BG in Y-axis) and (b) -12-05 (0-180 m BG in Y-axis) collected via dry sonic and air rotary drilling. Solid lines represent major grids for the x-axes. Vertical dashed lines represent instrument's (0.03 mg/L) and calculated (1.56 mg/L) method detection limits (MDLs) for dissolved porewater and porewater equivalent NO_3^--N concentrations, respectively.

Statistical summaries and box and whisker plot of NO_3^--N concentrations for squeezed porewater samples from fresh-blast (n=5) and waste rock (n=34) samples are presented in Table 3 and Figure 3, respectively. The dissolved median and mean NO_3^--N concentrations of squeezed fresh-blast and aged waste rock samples were 394 and 473±479 mg/L; and, 2.41 and 7.71±10.6 mg/L, respectively. The dissolved median and mean NO_2^--N concentrations of squeezed fresh-blast rock samples were 0.71 and 1.36±1.30 mg/L, respectively. The NO_2^--N concentrations of aged waste rock samples were below MDL for all but one sample (Table 4).

Comparison between porewater equivalent NO_3^--N concentrations (C_{pw}; mg/L) measured on aqueous leached samples and dissolved porewater NO_3^--N concentrations (C_S; mg/L) measured on squeezed samples from both fresh-blast and dump samples yielded a linear correlation (C_{pw} =0.8C_S +83; r^2=0.6; n=26). These results support the use of aqueous leach samples to estimate porewater NO_3^--N concentrations.

3.2. N Leached from Humidity Cells, Leach Pads, Boreholes and Rock Drain

The NO_3^--N concentrations in leach water from the HCs over 4.5 years of testing are presented in Figure 6a. The maximum NO_3^--N concentrations measured ranged from 4.7 to 35.5 mg/L. Cumulative mass of NO_3^--N released (ΣM) from each HC was calculated by adding the products of NO_3^--N concentration and water release data, and normalizing with respect to total NO_3^--N mass (*Mo*). These data are plotted vs. estimated pore volume flushed (*PVs*; the ratio of the cumulative volume of water release from the cell to initial VWC in the dump) in Figure 6b. Initial VWC of the waste rock samples was assumed to be 10% based on average GWC (5.2%) (Dawson, 1994; Dawson et al., 1998). The average density of 850 kg/m^3 were considered based on dimensions of HC filling of core waste rock samples. The sensitivity of the normalized mass release curves to estimates of calculated pore volume showed that increasing the initial VWC shifted the graph laterally (resulting in a *PV* offset) but did not alter the leaching efficiency (E_L; fraction of the solute mass initially present in the domain that was flushed after leaching one *PV*; Appels et al., 2016). The E_L was estimated by fitting equation (14) to observed $\Sigma M/M_0$ vs *PV* data:

$$\left(\frac{M}{M_0}\right) = 1 - (M_{PV-1} - M_{PV-1} \times E_L) \quad \ldots\ldots\ldots\ldots\ldots\ldots\ldots (14)$$

where M = mass released; PV=1 to N, where N= number of PVs needed to remove all NO_3^--N mass. At initial conditions when PV=0, there is no mass released and $M/M_0 = 0$.

The estimated E_L values for each HC based on fitting the early data ($M/Mo \leq 0.5$), varied from 0.07 to 0.40 with a mean value of 0.24±0.08. The maximum NO_3^--N concentration in the leach water was only measured after 8-10 PVs (data not shown), at which time the majority of the NO_3^--N mass (70- 80%) had been removed. Most of the NO_3^--N (95%) was removed from the HCs after 15-20 PVs. The total NO_3^--N mass released (Mo) from each cell reflects the initial NO_3^--N concentration (mg/kg). It ranged from 5.11 to 32.5 mg/kg with a median and mean value of 10 and 15±10 mg/kg, respectively (Table 5; Figure 6c). The NH_3-N concentrations in the leach water ranged from below MDL to 0.51 mg/L and the total NH_3-N mass released from each cell ranged from 0.20 to 1.21 mg/kg with a mean value of 0.71±0.40 mg/kg.

The NO_3^--N concentrations in the leach water from the LPs between April 2009 and December 2013 are presented in Figure 7a. These data showed progressive flushing of NO_3^--N with time, high during low flow time and vice versa. Peak NO_3^--N concentration decreased progressively after every flushing cycle and consistent with the HCs data. The ΣM, PV and E_L values were calculated following the procedure for the HCs described above. Initial VWC was considered to be 10% to measure initial volume of water in the waste rock based on average GWC of 5.2% (Barbour et al., 2016; Dawson, 1994). The average density of waste rock samples was considered to be 1900 kg/m^3 to measure volume of waste rock samples used for this experiment (Dawson, 1994; Dawson et al., 1998). Estimated E_L values for the LPs were 0.4, 0.4 and 0.45 (Figure 7b) with a mean value of 0.42±0.03. Maximum NO_3^--N concentrations in the LPs were variable (7, 62, and 175 mg/L) and were observed after 1- 2 PVs. The majority of the NO_3^--N was rapidly flushed from the LPs during the first 6-10 PVs. The initial NO_3^--N concentrations based on total mass release from the LPs were 0.78, 4.70 and 16.8 mg/kg with a median and mean values of 5 and 7±8 mg/kg, respectively (Table 5; Figure 7c). The maximum NO_2^-- and NH_3-N concentrations ranged from 0.08 to 0.34 and 0.12 to 0.24 mg/L, respectively. The total NO_2^-- and NH_3-N mass released from these three LPs was 0.003, 0.007 and 0.004 mg/kg; and 0.003, 0.012 and 0.001 mg/kg, respectively.

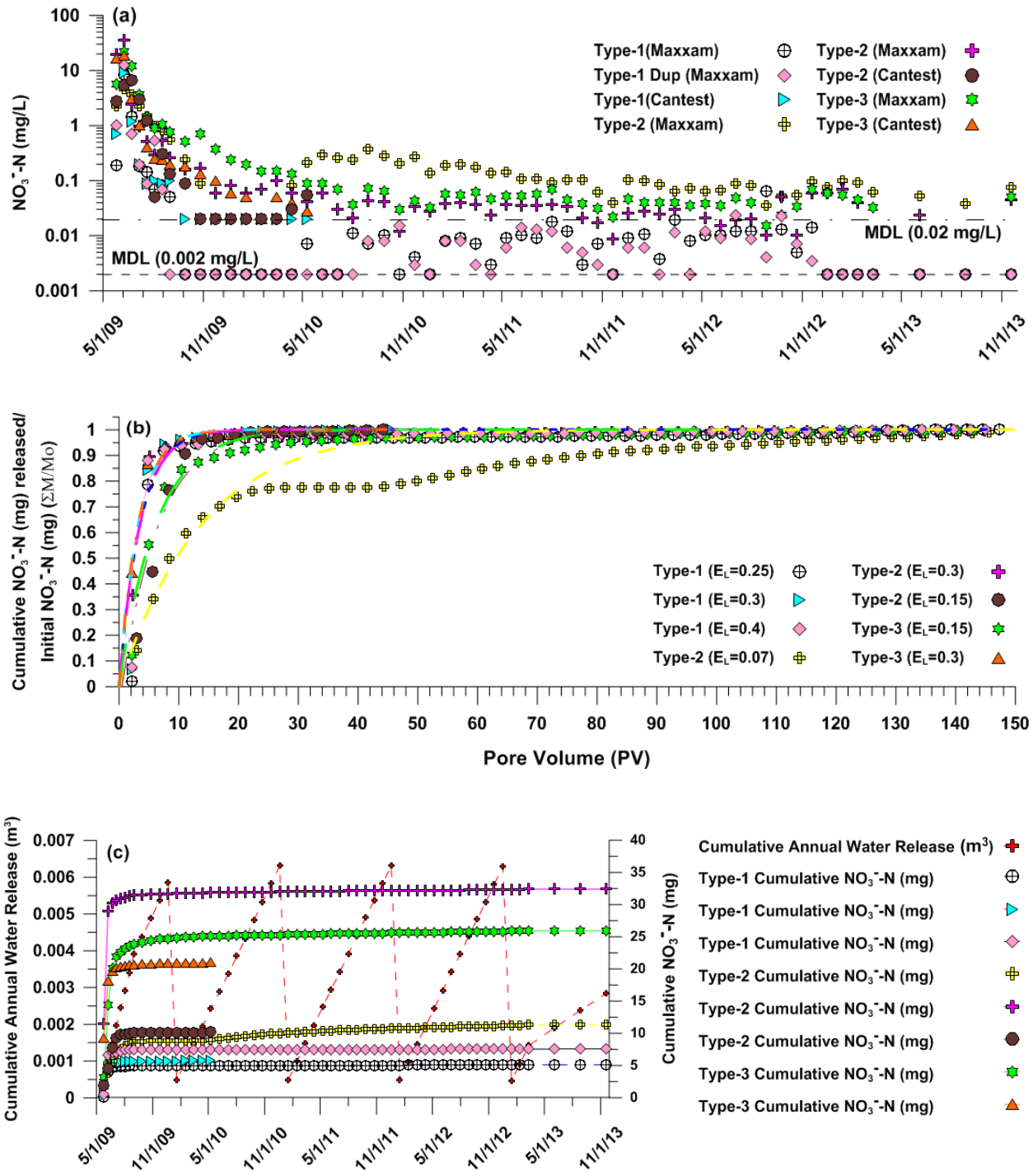

Figure 6. Results of HC tests: (a) time series of NO_3^--N flushed from cells (mg/L). Horizontal dashed lines represent method detection limits (MDLs) of 0.02 and 0.002 mg/L for two different analytical labs, Cantest and Maxxam, respectively; (b) changes in ΣM/Mo vs. pore volume flushed. The solid symbols represent the observed data and dashed lines represent the fitted constant leaching efficiencies (presented in brackets); and (c) cumulative annual water release

and cumulative NO_3^--N mass release with time. Cumulative annual discharge (m^3) is same for all HCs.

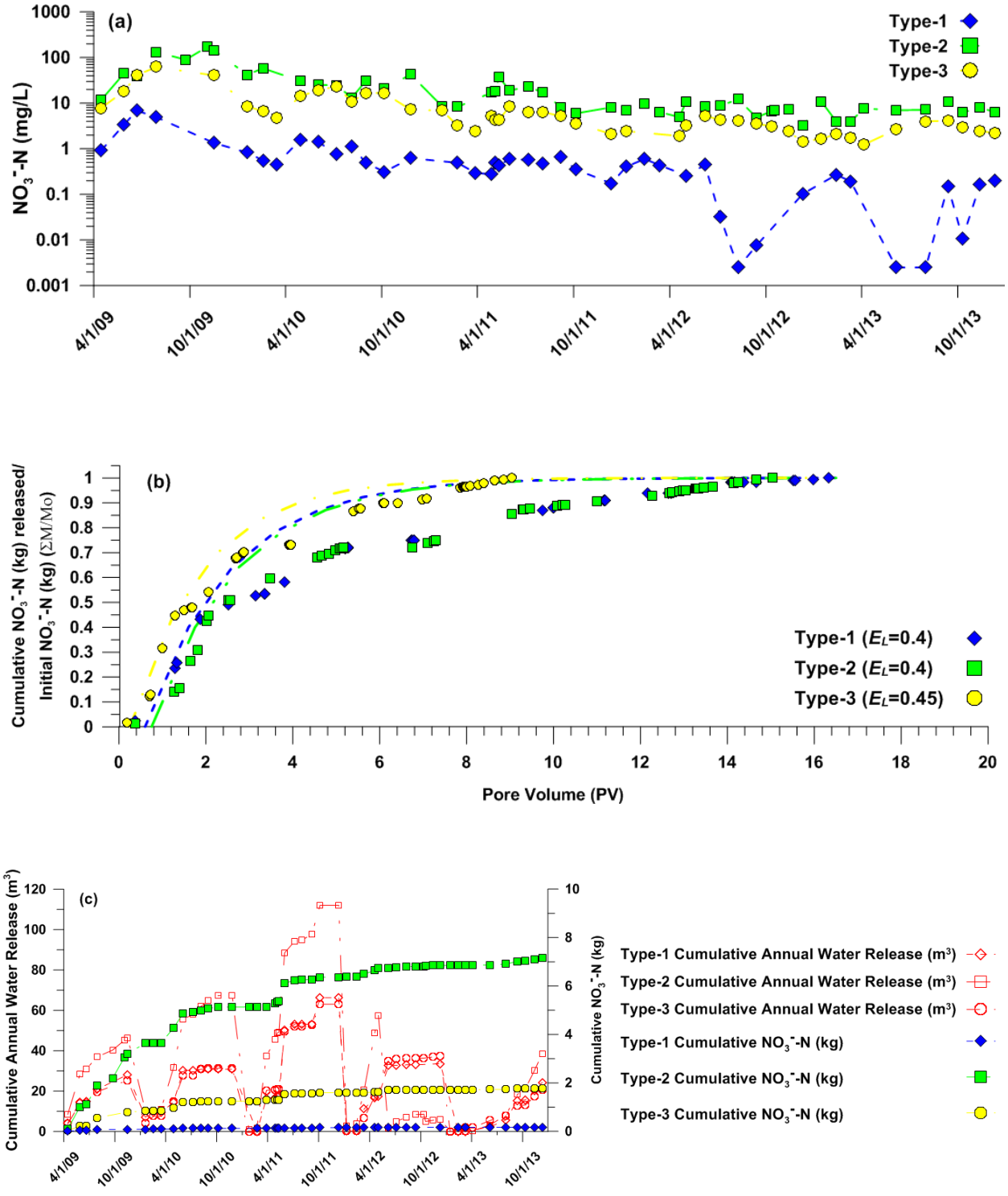

Figure 7. Results of Leach Pad tests: (a) time series of NO_3^--N flushed from LPs (mg/L); (b) changes in ΣM/Mo vs. pore volume flushed. The solid symbols represent the observed data and

dashed lines represent the fitted constant leaching efficiencies (presented in brackets); and (c) cumulative annual water release and cumulative NO_3^--N mass released with time.

Table 5: Summary of initial NO_3^--N concentration (mg/kg) and %Nloss from laboratory leach tests, humidity cell, and leach pad tests.

Fresh Waste Rock	NO_3^--N mg/kg	NO_3^--N loss kg/BCM	Total Nloss kg	%Nloss
FRO Fresh-blast rock (n=36)				
Median	**12.6**	**0.02**	**3.2E+04**	**3.40**
Mean	**27.6**	**0.05**	**7.0E+04**	**7.50**
Humidity Cells (HCs, n=8)				
Type-1 (Maxxam)	5.11	0.01	5.1E-06	1.39
Type-1 (Cantest)	5.73	0.01	5.7E-06	1.56
Type-1 (Dup: Maxxam)	7.56	0.01	7.6E-06	2.05
Type-2 (Maxxam)	11.4	0.02	1.1E-05	3.09
Type-2 (Dup: Maxxam)	32.4	0.06	3.2E-05	8.80
Type-2 (Cantest)	10.2	0.02	1.0E-05	2.76
Type-3 (Maxxam)	25.9	0.05	2.6E-05	7.04
Type-3 (Cantest)	21.0	0.04	2.1E-05	5.70
Median	**16.2**	**0.03**	**1.6E-05**	**4.39**
Mean	**14.9**	**0.02**	**1.5E-05**	**4.05**
Leach Pads (LPs, n=3)				
Type-1	0.78	0.01	0.17	0.21
Type-2	16.8	0.03	7.14	4.56
Type-3	4.70	0.01	1.76	1.27
Median	**4.70**	**0.01**	**1.75**	**1.27**
Mean	**7.43**	**0.01**	**2.51**	**2.01**

To estimate the E_L at the borehole scale, cumulative NO_3^--N mass release (ΣM) was quantified for LCO-WLC boreholes (12-02a, -05C_1 and -05C_2; Table 6). The remaining NO_3^--N mass for each borehole was calculated per unit area using NO_3^--N concentration (mg/kg), the thickness of each dump (m) and density of waste rock (1900 kg/m^3; Dawson, 1994; Dawson et al., 1998). The initial NO_3^--N concentrations of 10 and 15 mg/kg were considered (further discussed in section 4.1) to estimate total NO_3^--N mass release. A recharge rate of 500 mm/y (Barbour et al., 2016) and initial VWC of 10% (Barbour et al., 2016) were considered to calculate the number of PVs required to flush out a fraction of NO_3^--N mass from each borehole. Table 6 represents the number of PVs required to flush out a fraction of initial mass (*M/Mo*) from 12-02a, -05C_1 and -05C_2 respectively. These data suggest that the range of E_L at the dump scale ranged from 0.7 to 0.9 and the average is 0.8.

Table 6: Number of PVs required to flush out a fraction of mass (M/Mo) from LCO-WLC-12-02a, -05C1 and -05C2 respectively based on assumed recharge rate (500 mm/y) and initial VWC (10%) (Barbour et al., 2016).

Boreholes	**Assumed Recharge rate (mm/year)**	**Vol soil moisture**	**Profile thickness m**	**Number of Years**	***PV***	$M_{release}/Mo$ **(Mo = 15 mg/kg)**	$M_{release}/Mo$ **(Mo = 10 mg/kg)**
LCO-WLC-12-02	500	0.1	83	22	1.33	0.80	0.70
LCO-WLC-12-05C1	500	0.1	164	34	1.04	0.90	0.85
LCO-WLC-12-05C2	500	0.1	177	34	0.96	0.90	0.85

The NO_3^--N time series (1993-2014) for the rock drain and ΣM for NO_3^--N released from the dump to the rock drain are presented in Figure 8. The annual maximum NO_3^--N concentration has increased noticeably since 2000 and peaked during winter base flow, 2007 (~50 mg/L), 25 years after dumping began. Since 2007, the annual peak NO_3^--N concentrations have progressively decreased. However, the peak concentration of the most recent year is still higher than 2000. Seasonal effects of dilution (spring thaw), i.e. low NO_3^--N concentration during high flow and vice versa were observed in the WLC rock drain data. Relatively high NO_3^--N concentrations (40±12 mg/L) were measured during low base flow condition while high flow spring freshet periods contain low NO_3^--N concentrations (10-15 mg/L). The pre- and post-2000 cumulative annual NO_3^--N flux from the dump were approximately 1.5×10^4 and 5.2×10^4 kg/year, respectively and the ΣM for NO_3^--N flushed from the dump since 1982 was estimated to be 1.1×10^6 kg.

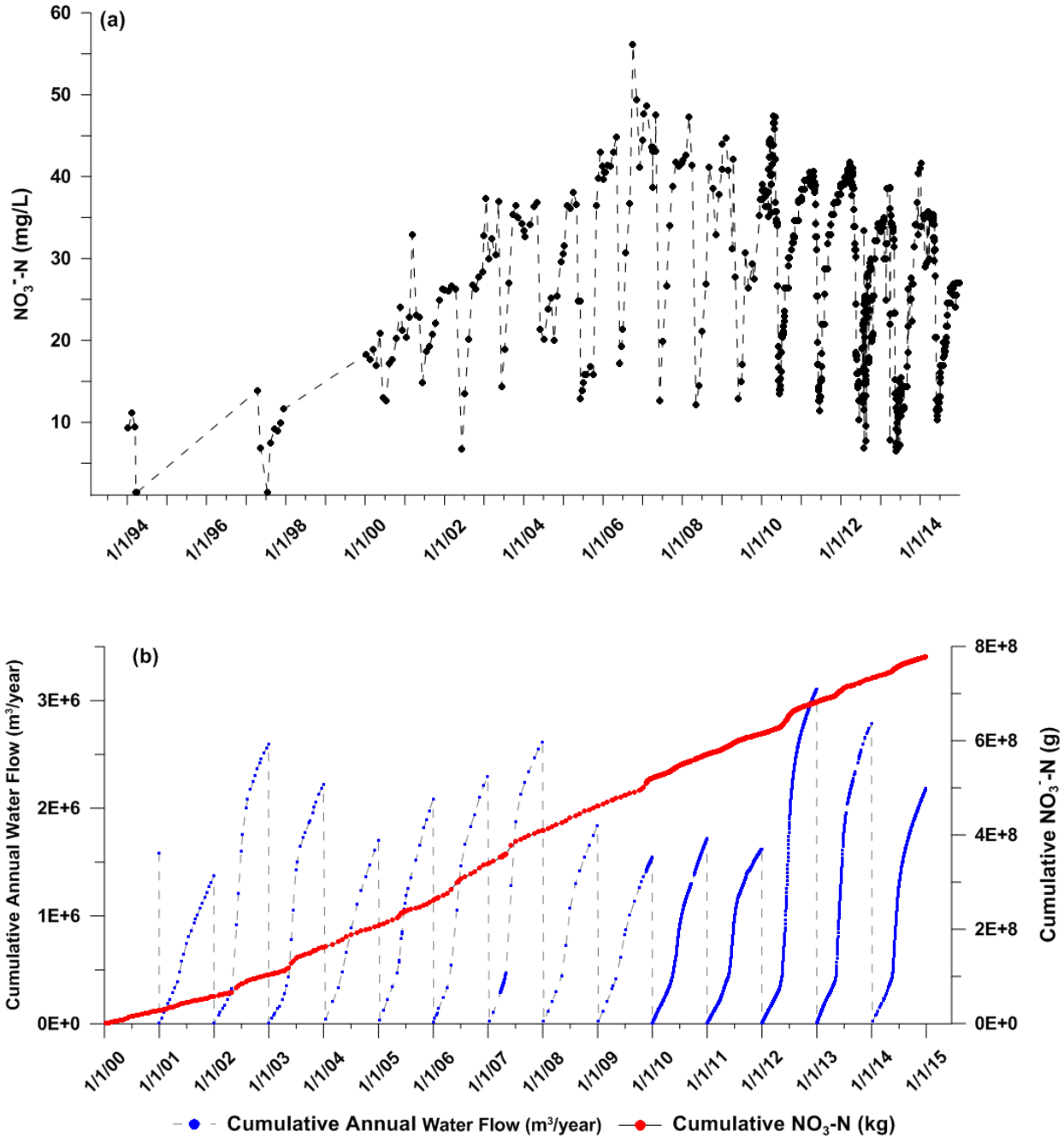

Figure 8. Results of WLC rock drain: (a) time series of NO_3^--N flushed (mg/L); (b) cumulative annual water flow and cumulative NO_3^--N mass release with time.

3.3. O_2 Gas Concentrations

O_2 gas concentrations measured in CMTs vs. depth in the dump at both drill sites are presented in Figure 9. These data showed that zones of oxygen depletion (sub oxic condition) exist in the dump and the O_2 concentrations in these zones can be transient.

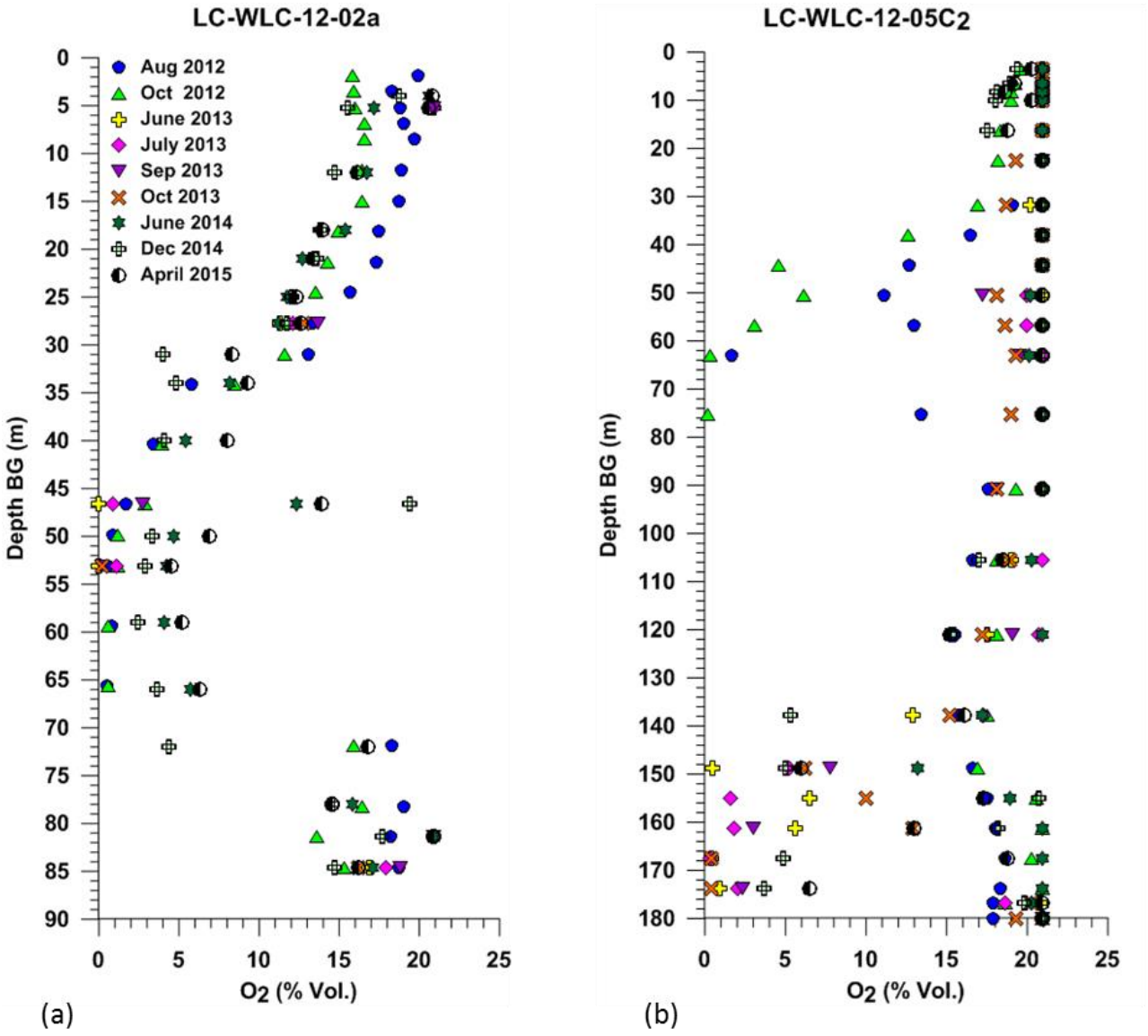

Figure 9. Pore-gas O_2 concentration (vol.%) collected between August 2012 and April 2015 vs. depth at (a) LCO-WLC-12-02a (0-90 m BG in Y-axis) and (b) -12-05C_2 (0-180 m BG in Y-axis).

In general, O_2 concentrations at 12-02a, decreased from atmospheric (21 vol.%) at the ground surface to 5-8 vol.% at 34 m BG (Figure 9a) and remained at < 5 vol.% between 40 to 66 m BG. Below 66 m, the concentrations increased to > 13 vol.% from 72 to 85 m BG. The transient nature of the O_2 is reflected in data collected at 47 m BG. At this depth, the O_2 concentrations increased from 0.2 vol.% (approaching anoxic conditions) on August 2012 to 20 vol. % (oxic) on April 2015. This zone was sub-oxic (O_2 concentration < 5 vol.%) until October 2013. After June 2014, the O_2 in this zone reflected oxic conditions (O_2 concentrations > 15 vol.%). At 12-05C_2, the O_2 concentrations were consistently > 15 vol.% throughout the profile with the exception of two depths from 40-80 and 135-175 m BG (Figure 9b). In these zones, O_2 decreased to <5 vol.% for short periods of time. From August to October 2012, the O_2 concentrations between 40 and 60 m BG were <5 vol. % but increased >15 vol.% between June 2013 and April 2015. Between 135 and 175 m BG, the O_2 decreased from >15 vol. % to < 5 vol.% from June 2013 to October 2013. The increased O_2 concentrations at the base of both sites may be attributed to the lateral convective transport of atmospheric air through the coarse rock at the base of the dump. In contrast, the O_2 values measured at all gas ports in each LPs were similar to atmospheric conditions (~ 20 vol. %) throughout the testing period.

3.4. Isotope Analyses of N Species

The δ^{15}N-total N analyses of the Mist Mountain source rock (n=7) yielded δ^{15}N values that ranged from 2.2 to 4.4‰. A cross-plot of $\delta^{15}N\text{-}NO_3^-$ vs. $\delta^{18}O\text{-}NO_3^-$ of aqueous samples from NH_4NO_3 (the ANFO prill; n=1), the FRO-TCR fresh-blast rock (n=4), LCO-WLC unsaturated waste rock (n=33) and WLC rock drain samples (n=12) is presented in Figure 10. The $\delta^{15}N\text{-}NO_3^-$ and $-NH_4$ and $\delta^{18}O\text{-}NO_3^-$ values of the ANFO prill were 4.3‰, -0.6‰ and 24.9‰, respectively. $\delta^{15}N\text{-}NO_3^-$ values of most leached samples from dump (29 of 33 samples analyzed) and rock drain samples ranged from +0.63 to +7.23‰. Unlike the $\delta^{15}N\text{-}NO_3^-$ values, $\delta^{18}O\text{-}NO_3^-$ values of these samples were more depleted (-10.4 to +15.7‰) than the ANFO prill (+24.9‰). δ^{15}N- and $\delta^{18}O\text{-}NO_3^-$ values of fresh-blast samples ranged from +0.61 to +3.34‰ and +21.3 to +26.6‰, respectively. Overall a lack of δ^{15}N- and $\delta^{18}O\text{-}NO_3^-$ enrichment was observed in most samples. However, minimal enrichments of δ^{15}N- and $\delta^{18}O\text{-}NO_3^-$ were measured for few leached (n=4) and rock drain (n=4) samples. The leached samples were collected from 26 and 57

m BG at 12-02 and 40 and 80 m BG at 12-05; and yielded δ^{15}N- and δ^{18}O-NO_3^- values that ranged from +11.4 to 15.8‰ and -2.49 to +3.42‰, respectively. These enriched leached samples were collected from sub-oxic zones in the dump.

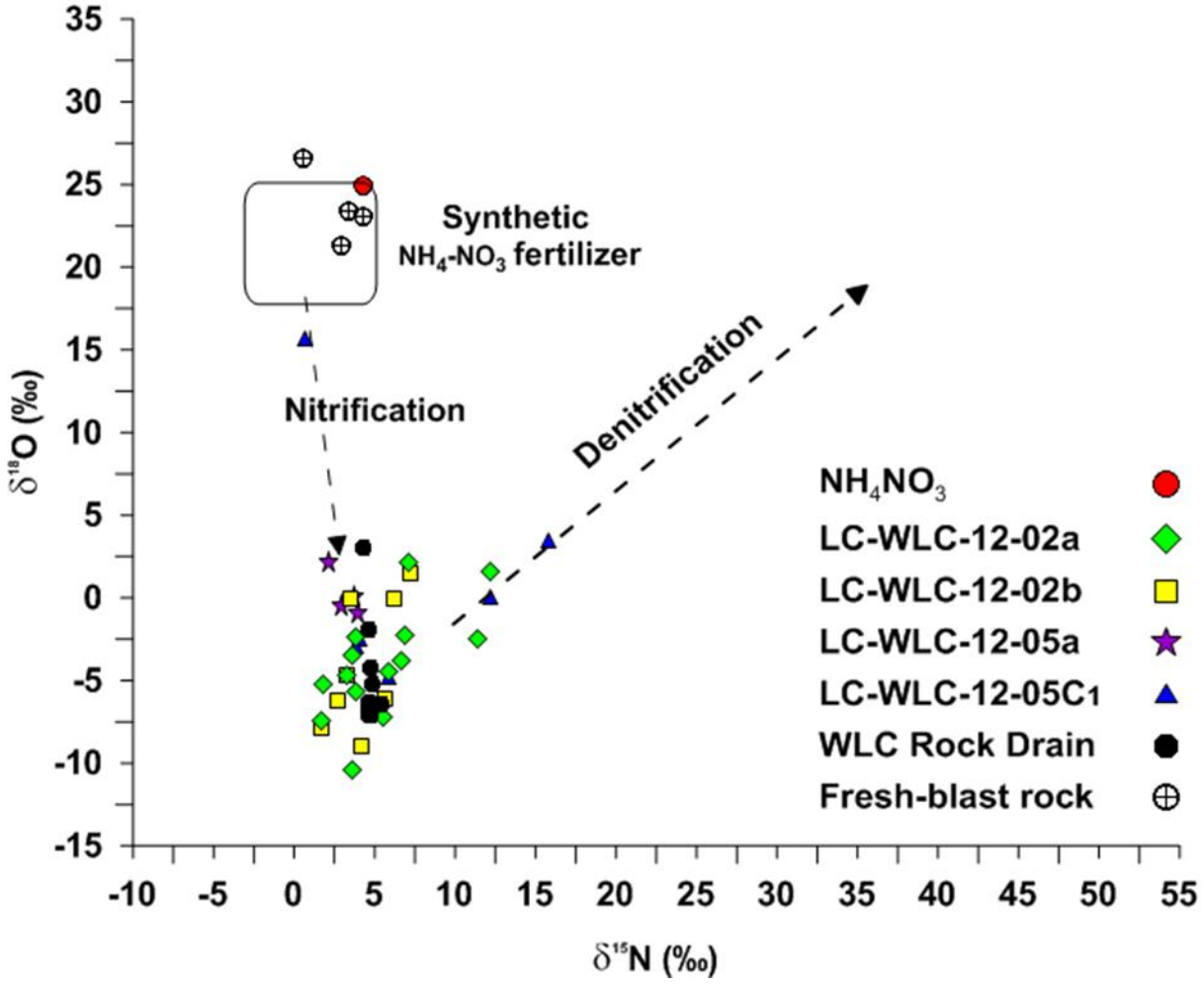

Figure 10. δ^{15}N-NO_3^- vs δ^{18}O-NO_3^- of water samples from NH_4NO_3 (ANFO prill), fresh-blast rock (FRO-TCR), LCO-WLC waste rock dump and WLC rock drain samples. The box represents the ranges of existing δ^{15}N- and δ^{18}O-NO_3^- data for synthetic NH_4NO_3 fertilizer (Hübner, 1986; Macko and Ostrom, 1994; Clark and Fritz, 1997; Kendall et al., 1998).

4. DISCUSSION

4.1. Source and Initial Concentrations of N in Waste Rock

Chemical analyses of freshly blasted (i.e., fresh-blast rock and HC and LP test samples) and aged waste rock (waste rock samples from LCO-WLC boreholes deposited between 1982 and 2012) samples show the dominant form of N in the dump is NO_3^--N. The porewater equivalent NO_3^--N concentrations in the fresh-blast and aged waste rock samples ranged from 0.78 to 4343 mg/L (median and mean of 227 and 497±854 mg/L) and 0.78 to 486 mg/L (median and mean of 22.2 and 48.3±78.9 mg/L), respectively. In contrast to NO_3^--N, porewater equivalent NO_2^--N concentrations in the fresh-blast and aged waste rock samples as well as LPs were below MDL (except one in aged waste rock, 3.56 mg/L) and represent as a minor N species. The presence of low NH_3-N concentrations in the HCs (below MDL to 0.51 mg/L) and LPs (below MDL to 0.24 mg/L) tests relative to NO_3^--N concentrations in the HCs (below MDL to 35.5 mg/L) and LPs (below MDL to 175 mg/L) also suggest that NH_3-N is also a minor N species in the waste rock samples.

Several lines of evidence identify the source of the NO_3^--N in the waste rock to be blasting (i.e., ANFO). Leachable concentrations of NO_3^--N in fresh-blast rock (median=12.6 mg/kg) and concentration of NO_3^--N in fresh waste rock used in the HCs and LPs (median values of 16.2 and 4.70 mg/kg, respectively) were much greater than in pre-blast rock (mean=0.20±0.10 mg/kg). In addition, the similarity between the δ^{15}N- and δ^{18}O-NO_3^- from fresh-blast rock and a sample of ANFO is consistent with high NO_3^--N concentration in fresh-blast rock being derived from ANFO. The isotopic values for δ^{15}N-NO_3^- and -NH_4^+ values of an ANFO prill (+4.29 and -0.61‰, respectively) were also consistent with δ^{15}N-NO_3^- and -NH_4^+ values from synthetic NH_4NO_3 fertilizer that ranged between -6.00 and +6.00‰ and -0.91 and ±1.80‰, respectively (Hübner, 1986; Macko and Ostrom, 1994; Clark and Fritz, 1997; Kendall et al., 1998). In addition, the δ^{18}O-NO_3^- value of the ANFO prill (+24.97‰) was consistent with values from synthetic fertilizer in which the majority of the O_2 in the NH_4NO_3 is derived from the atmosphere (δ^{18}O value of +23.5‰; Kroopnick and Craig, 1972; Horibe et al., 1973).

The NO_3^--N concentrations attributed to blasting were highly variable within and between the HC and LP datasets and the fresh-blast waste rock samples. This variability in fresh waste rock can be attributed to a number of compounding factors including differences in

blasting efficiencies between blast holes, spilling of explosives during loading or transportation, dissolution of explosives by water in the blast holes, infiltration of undetonated explosives from the blasted muck and proximity of the solid sample locations to blast holes, or a combination of these (Cameron et al., 2007; Bailey et al., 2013; Pommen, 1983).

A summary of initial NO_3^--N concentration and %N loss (i.e., residual N discharge from undetonated explosives remaining on the waste rock after the blasting) from aqueous leached, HC and LP tests is presented in Table 5. However, it was assumed that the residual N discharge from undetonated explosives was similar at each operation site (LCO and FRO) and within an individual site for rock blasted at different times. Based on leachable median and mean NO_3^--N concentrations from fresh-blast and fresh waste rock used in the HCs and LPs, initial NO_3^--N concentrations range from 5-28 mg/kg. The variability in measured concentrations of freshly blasted rock suggests a range of initial NO_3^--N concentrations for individual dump constructed from the Mist Mountain Formation. The median NO_3^--N concentration of fresh-blast, HCs and LPs waste rock were 12.6, 16.9 and 4.7 mg/kg, respectively. Based on our data for fresh waste rock (median NO_3^--N concentration), the initial NO_3^--N concentration should lie between 10 and 15 mg/kg. This equates to porewater equivalent concentration of between 190 and 285 mg/L, calculated using waste rock density and VWC of 1900 kg/m^3 and 10%, respectively, (Dawson, 1994; Barbour et al., 2016).

%N losses were calculated based on waste rock volume of FRO-TCR (1.35×10^6 BCM), HCs and LPs as well as powder factor (~0.7) used in the Teck coal mining operation (CMJ, 2000). The median concentration of NO_3^--N in the fresh-blast rock and the HCs and LPs equates to 3.4, 4.4 and 1.3% N losses from explosives. These values for fresh-blast, HCs and LPs are consistent with the N losses estimated using equation presented in Ferguson and Leask (1988) and calculated by LCO explosive recipe data for 1993-2010 (Table 7). Based on assumed %N loss from ANFO and emulsion after the detonation of 0.10% and 8.50%, respectively (Ferguson and Leask, 1988), the calculated %N loss from explosive residues was estimated to range from 1.4 to 2.9% (Table 7). The measured data are consistent with N losses reported by Pommen (1983) and Bailey et al. (2013). Pommen (1983) determined the N loss to range from 0.1 to 6% from a field-based study conducted on waste rock in the Elk Valley. Bailey et al. (2013) reported the N loss of 5.4% from laboratory leach tests on freshly blasted rocks and 5.6% from large-scale

test piles conducted at the Diavik Diamond mine, Northwest Territories, Canada operated by Diavik Diamond Mines Inc.

Table 7: NO_3^--N, NH_4^+-N, and NO_2^--N loss from Line Creek Operation (LCO) from ANFO from 1993-2010.

Year	Total N_{loss}* kg	N_{loss}/N_{total} %	N_{loss} by compounds (kg)* NO_3^--N	NH_4^+-N	NO_2^--N	NO_3^--N** (mg/kg rock)
1993	65501	1.44	56985	6550	1710	1.85
1994	71083	1.44	61842	7108	1855	1.85
1995	74273	1.44	64618	7427	1939	1.85
1996	84189	1.44	73244	8419	2197	1.82
1997	89964	1.44	78268	8996	2348	1.81
1998	91112	1.44	79267	9111	2378	1.8
1999	81408	1.44	70825	8141	2125	1.8
2000	88984	1.44	77416	8898	2322	1.77
2001	111325	1.44	96853	11133	2906	1.76
2002	127635	1.44	111043	12764	3331	1.75
2003	87388	1.44	76028	8739	2281	1.73
2004	73246	1.44	63724	7325	1912	1.79
2005	156227	2.92	135918	15623	4078	3.46
2006	143848	2.92	125147	14385	3754	3.48
2007	138115	2.92	120160	13811	3605	3.48
2008	177222	2.92	154183	17722	4625	3.4
2009	154832	2.92	134704	15483	4041	3.39
2010	199698	2.92	173737	19970	5212	3.33
Mean	112003	1.93	97442	11200	2923	2.34

* Calculated from Ferguson and Leask, (1988)

** Estimated LCM (loose cubic meter) density = 1900 kg/m^3

4.2. Geochemical Controls on Nitrate in the Dump

The $\delta^{18}O$ values of NO_3^--N leached from the dump samples and WLC rock drain samples exhibited evidence of nitrification ($NH_4^+ \rightarrow NO_3^-$; Figure 10) when compared to values from the fresh-blast and ANFO samples. The $\delta^{18}O$-NO_3^- data of the dump (-10.4 to +15.7‰) and WLC rock drain (-7.06 to +3.06‰) were considerably more depleted compared to that of ANFO (+25‰). This isotopic shift can be explained as a result of nitrification and is consistent with the literature. Based on soil incubation experiments, Amberger (1987) suggests that NO_3^- produced by nitrification could have negative $\delta^{18}O$ values. Further, Voerkelius and Schmidt (1990) published data on $\delta^{18}O$ values of 0±2‰ for microbial NO_3^- generated in soil column

experiments. More recently, laboratory soil incubation studies showed $\delta^{18}O$ values of between +2 and +17‰ can be attained from the nitrification processes (Kendall, 1998). These data suggest that some of the NO_3^- in the dump is derived from nitrification of NH_4^+ (integral part of ANFO).

Oxygen gas concentrations vs. depth profiles show that sub-oxic conditions (0.2-10.9 vol.%.) exist in localized zones within the dump (Figure 9). Their presence can be attributed to variability in the local environment such as finer textured zones resulting in increased moisture contents and reduced O_2 diffusion (Bernstein et al., 2013; Nicholson et al., 1989). In oxygen-depleted zones, NO_3^- can serve as a secondary oxidant and can undergo denitrification. The presence of high dissolved NO_3^--N concentrations in the zones at 12-02a and 12-05C2 in which O_2 concentrations vary (e.g., 26-70 m BG at 12-02a; 40 and 75 m BG at 12-05C2; Figure 9) is not suggestive of notable denitrification (Figure 4; Figure 5). However, a slight enrichment in $\delta^{15}N$- and $\delta^{18}O$-NO_3^- values of four water extractable samples (ranging from +11.4 to 15.8‰ and -2.49 to +3.42‰, respectively) from a zone of low O_2 concentrations may reflect the presence of minor denitrification in the waste rock dump. Overall, our data suggest limited to no denitrification occurs in the dump and, as such, NO_3^- can be considered to be a conservative species.

4.3. Distribution and Concentrations of N in the Dump

Nitrate-nitrogen concentrations in the dump are lower (median=1.26 mg/kg; mean=2.43±3.81 mg/kg) than in fresh-blast rock (median=12.6 mg/kg; mean=27.6±47.4) and exhibited considerable sample-to-sample variability (Figure 4; Figure 5). This variability can be attributed to concentration variations in the waste rock during deposition (discussed above) or variable rates of flushing of the NO_3^--N due to textural heterogeneity in the dump. Results of Student's t tests between NO_3^--N data of each borehole from LCO-WLC dump and pre-blast samples (MM1306) are presented in Table 8. With the exception of pre-blast samples, statistical results showed no significant difference between samples from different sampling methods (sonic and air rotary) from the same location (e.g. 12-05a vs 12-05C1) but exhibited differences between samples of different locations (e.g. 12-02a vs 12-05C1, 12-02a vs 12-05C2). The statistical differences between the samples from the dump <40 m bgs and >40 m bgs, 12-05C1 or 12-05C2 were attributed to flushing of NO_3^--N from the WLC dump since deposition.

Table 8: Results of Student's t tests on water extractable NO_3^--N concentrations (mg/kg) in waste rock samples from different boreholes and pre-blast rocks (MM1306).

	12-02	12-02 (< 40 m bgs)	12-02 (>40 m bgs)	12-05a	12-05C1	12-05C2	Pre-blast MM1306
12-02 (n=85)	X	**0.0006**	**0.0003**	0.1753	**0.0013**	**0.0445**	**4.76E-12**
12-2 (< 40 m bgs) (n=58)		X	**1.41E-09**	**0.0145**	**1.60E-09**	**4.28E-11**	**9.59E-22**
12-2 (>40 m bgs) (n=27)			X	0.6948	0.7463	**0.0153**	**0.0027**
12-05a (n=12)				X	0.8224	0.5179	**0.0098**
12-05C1 (n=51)					X	**0.0499**	**0.0011**
12-05C2 (n=57)						X	**7.12E-11**
Pre-blast (n=22)							X

Notes: Values in brackets represent the number of samples analyzed. Bold values reflect a difference detected at a 95% confidence interval (p-value < 0.05).

4.4. NO_3^- Flushing

Insights into the flushing behavior of NO_3^- through the dump were obtained from the smaller scale HCs and LPs experimental data. The NO_3^- removal process is controlled by the E_L associated with NO_3^- mass release *(M)* and PVs at each flushing cycle. The number of PVs needed to attain peak NO_3^- concentrations in the effluent decreased with increasing volume of waste rock material tested. For example, peak NO_3^- concentrations were observed at 5- 6 PVs at the small scale (1 kg) HCs while only 1-2 PVs were needed for the LPs (213-425 kg). Further, the peak NO_3^- concentrations measured at the WLC rock drain were observed between 2006 and 2009 at PV< 1.

The average estimated E_L for HCs and LPs were 0.2 and 0.4 respectively. At the borehole scale, total NO_3^--N flushed out from the dump with leaching efficiencies between 0.7 and 0.9 with an average of 0.8 and is consistent with Appels et al. (2016) where E_L were estimated for waste rock dumps using numerical simulations run under numerous combinations of textural, structural and moisture heterogeneity. The E_L of HCs, LPs and borehole scale increased with the volume of waste rock materials contained in each. The E_L is expected to be equal to 1 in the case of uniform matrix flow. However, it will be less than 1 if there are zones of stagnation or macro-pores that facilitates the by-pass or divergence of flow, resulting in the presence of residual mass remaining in the no flow zone of the unsaturated medium (Appels et al., 2016; Eriksson et al., 1997; Amos et al., 2015). The lower E_L and higher PVs for most NO_3^- mass removal from HCs suggest the dominance of macro-pore or preferential flow. The use of loose waste rock with lower density (850 kg/m^3), poorly sorted grain size distribution (< 6.5 mm), and lack of compaction might create a conducive condition for preferential flow in HCs. The higher E_L of LPs might be due to more influence of matrix flow and less of preferential flow in the waste rock materials with respect to HCs. Our findings at the LP scale are consistent with Neuner et al. (2013), in which matrix flow was suggested as a major flow mechanism in a lysimeter experiment. In contrast, Nichol et al. (2005) stated that preferential and non-capillary flow dominated in a 5 m high waste rock pile and were attributed to the coarse but poorly sorted particles ranging from 1.5 m to clay size. At the borehole scale, the high E_L is an indicator of the dominance of matrix flow over preferential flow across the waste rock dump. Since 1 PV of

water is capable of flushing ~80% of the initial NO_3^- mass over the 34 years, it will take at most 40 to 60 years to flush 99% of NO_3^- from the waste rock dump.

The current study reveals that the scale dependency of E_L is associated with the rock volumes in a way that NO_3^- from larger waste rock volume can be flushed more efficiently. The scale dependency of E_L from the current research disagrees with the findings of Eriksson et al, (1997) where they reported matrix flow control at the laboratory scale and the influence of preferential at the field scale. Differences in waste rock properties between (e.g. grain size, compaction and sorting) the two studies may be the reason for the varying results. Such scale dependency in the current study indicates the dominance of preferential flow at smaller scales, while matrix flow exerts strong influence at the field-scale. As a result, a shift from preferential flow to matrix flow dominated system is observed as the transportation medium scales up.

Assuming initial NO_3^--N concentration of 10 to 15 mg/kg (discussed above) and the volume of WLC waste rock dump (2.1×10^8 BCM), 20 to 30% of NO_3^--N has been flushed from the WLC rock drain since dump construction (1982) with the remaining (3×10^6 to 5×10^6 kg of NO_3^--N) in the dump.

5. SUMMARY AND CONCLUSIONS

The goal of this thesis was to investigate the source and fate of NO_3^- derived from blasting residuals in an unsaturated waste rock dump. Specific objectives were to: i) define the source of nitrate (i.e. geologic, blasting and/or oxidation of blasting residuals); ii) quantify initial NO_3^--N concentration in the waste rock dump; iii) identify factors that control the fate of NO_3^- (geochemical or physical) in the waste rock dump; and iv) characterize the long-term leaching of the NO_3^- from the waste rock dump.

The summaries and conclusions of this study include:

1. The NO_3^--N concentrations in post-blasting rock were greater than pre-blast rock. They are also statistically different. Pre-blast vs. fresh-blast rock and stable isotope data show that the NO_3^- in the waste rock dump is derived from blasting and oxidation of blasting residuals (i.e. nitrification).
2. Initial NO_3^--N concentrations ranged from 10-15 mg/kg which equates to porewater equivalent concentration of 190-285 mg/L.
3. The distribution of NO_3^- concentrations are highly variable, reflecting the physical heterogeneity of waste rock in the dumps. However, patterns of NO_3^- concentrations with depth exhibit effects of flushing.
4. Denitrification is limited in the unsaturated waste rock dump. As such, NO_3^- in this waste rock dump can be used as a tracer to determine water flushing efficiency and migration of water through the dump.
5. E_L is scale dependent (volume of waste rock), suggesting the dominance of preferential flow at the smaller scale and matrix flow at the field scale. The E_L at three different scales were determined to range from 15-30%, 40-45%, and 70-90% for the humidity cells, leach pads and WLC boreholes, respectively.
6. Scale dependency of E_L indicates that the findings from smaller scale experiments (HCs and LPs) may not be scaled to the field full scale dump, but can be valuable for understanding the flushing mechanism of NO_3^- from the dump.

6. RECOMMENDATIONS FOR FUTURE WORK

Findings of this thesis have improved current understandings on the source, geochemical controls, and flushing mechanism of NO_3^- in the waste rock dump. Although, this study used comprehensive datasets that provided high resolution NO_3^- data at multiple scales as well as stable isotopes measurements of δ^{15}N-TN, δ^{15}N-NH_4^+, δ^{15}N- and δ^{18}O-NO_3^-, there are some limitations in the methodology and datasets used in this study. These limitations indicated the following areas as recommendations for future work:

1. The current study is based on five boreholes drilled at two locations (the northern and southern part of the WLC dump) that provide dump chronology and geochemistry data. As a result, a comprehensive understanding regarding the inherent heterogeneity across the dump and its potential impacts on NO_3^- geochemistry and flushing is partly understood. Thus, additional boreholes distributed across the dump are recommended with high resolution sampling.

2. Characterization of the initial NO_3^--N concentration in the fresh waste rock is uncertain as the observed initial NO_3^--N concentration provide a wide range of variability. Since the mass of explosive used for blasting was not available, it was difficult to address this uncertainty. To better characterize the initial NO_3^- concentration in fresh waste rock, it is recommended that the mass of the loaded explosives be measured.

3. Waste rock and fresh-blast rock samples were collected from two different operation sites, LCO-WLC and FRO, respectively. In this study, we assumed that LCO-WLC and FRO samples were comparable with respect to blasting conditions (wet vs. dry) despite they were from two different sites. For future study, it is recommended to conduct a follow-up study on blasting condition/products to examine the comparability between waste rock and fresh-blast samples.

4. Geochemical data reported in this study are mainly from water extractable samples (aqueous leached) and a limited number of dissolved porewater samples (n=26). Though porewater equivalent NO_3^--N concentrations measured on aqueous leached samples and dissolved porewater NO_3^--N concentrations measured on squeezed samples from both fresh-blast and dump yielded a linear correlation, it is recommended to collect more dissolved porewater samples to increase the confidence level of using water extractable samples to estimate porewater NO_3^--N concentrations.

5. Measurement of N species in the leached and dissolved porewater samples only included NO_2^- and NO_3^-. It is recommended that all nitrogen species, including NO_2^-, and NO_3^-, and NH_4 be measured to determine total N mass in the water samples.

6. The dual isotope analyses on NO_3^- presented in this study showed that there was limited to no denitrification in the dump. However, the application of selenium geochemistry and isotope analyses would be helpful to understand whether selenate was reduced or not in the zone of limited denitrification. Thus, the measurement of selenate isotope ratio is recommended for a more robust conclusion on potential reduction processes.

7. REFERENCES

Amberger, A., 1987. Natural ^{15}N- and ^{18}O-NO_3^- contents as indicators of the origin of nitrate in soil and groundwater, Ph.D. Dissertation, Tech. Univ. München, 104 pp.

Amberger, A., Schmidt, H.-L., 1987. Natural isotope abundance of nitrate as an indicator of its origin. Geochimica et Cosmochimica acta. 51, 2699-2705.

Amos, R.T., Blowes, D.W., Bailey, B.L., Sego, D.C., Smith, L., Ritchie, A.I.M., 2015. Waste-rock hydrogeology and geochemistry. Applied Geochemistry. 57, 140-156.

Anderson, K. K., Hooper, A. B., 1983. O_2 and H_2O are each the source of one O in NO_2 produced from NH3 by Nitrosomas 15N-NMR evidence. FEBS Letters. 64, 236-240.

AMEC Environmental & Infrastructure, 2013. West Line Creek Groundwater Study & Conceptual Freshwater Diversion Options. Medicine Hat, AB: AMEC Americas Limited.

Appels, W., Ireson A.M., Barbour S.L., 2016. Impact of textural and structural heterogeneity on unsaturated flow and transport through mine waste rock. Vadose Zone Journal (Under Review).

ASTM D2216-10, 2010. Standard Test Methods for Laboratory Determination of Water (Moisture) Content of Soil and Rock, in: Annual Book of ASTM Standards, West Conshohocken, PA, 2010.

Aravena, R., Robertson, W.D., 1998. Use of multiple isotope tracers to evaluate denitrification in ground water: study of nitrate from a large-flux septic system plume. Groundwater. 36, 975-982.

Bailey, R.T., Hunter, W.J., Gates, T.K., 2012. The influence of nitrate on selenium in irrigated agricultural groundwater systems. Journal of Environmental Quality. 41(3), 783-792.

Bailey, B.L., Smith, L.J., Blowes, D.W., Ptacek, C.J., Smith, L., Sego, D.C., 2013. The Diavik Waste Rock Project: Persistence of contaminants from blasting agents in waste rock effluent. Applied Geochemistry. 36, 256-270.

Barbour, S.L., Hendry, M.J., Carey, S.K., 2016. High-Resolution Profiling of the Stable Isotopes of Water in Unsaturated Coal Waste Rock. Journal of Hydrology. 534, 616–629.

Benson, S.J., Lennard, C.J., Maynard, P., Hill, D.M., Andrew, A.S., Roux, C., 2009. Forensic analysis of explosives using isotope ratio mass spectrometry (IRMS)—Preliminary study on TATP and PETN. Science and Justice. 49, 81–86.

Bernstein, N. 2013. Effects of salinity on root growth, in: Eshel, A., Beeckman, T. (Eds.), Plant Roots: The Hidden Half. CRC Press, Boca Raton, Florida, 784 pp.

Biswas, A., Hendry, M. J., Essilfie-Dughan, J., 2016. Abundance and mineralogical associations of arsenic in coal waste rock, Elk Valley, British Columbia, Canada: Implications for arsenic mobilization in low sulfide - high carbonate waste rock. Int. J. Coal Geol. (*In Review*).

Bohlke, J.K., Mroczkowski, S.J., Coplen, T.B., 2003. Oxygen isotopes in nitrate: new reference materials for ^{18}O: ^{17}O: ^{16}O measurements and observations on nitrate-water equilibration. Rapid Communication in Mass Spectrometry. 17, 1835-1846.

Cameron, A., Corkery, D., MacDonald, G., Forsyth, B., Gong, T., 2007. An investigation of ammonium nitrate loss to mine discharge water at diavik diamond mines, in: EXPLO 2007 – Blasting: Techniques and Technology, Proc.; Wollongong, NSW. Australasian Institute of Mining and Metallurgy Publication Series, 21–33.

Casciotti, K.L., Sigman, D.M., Galanter Hastings, M., Böhlke, J.K., Hilkert, A., 2002. Measurement of the oxygen isotopic composition of nitrate in seawater and freshwater using the denitrifier method. Analytical Chemistry. 74, 4905-4912.

Clark, M.J.R., Peppin, P.A., 1984. A Trend Study of Water Quality in British Columbia. Waste management Brunch, B.C. Ministry of Environment, 75 pp.

Clark, I. D., Fritz, P., 1997. Environmental Isotopes in Hydrogeology. CRC Press, Boca Raton, FL.

Comly, H. H., 1987. Cyanosis in Infants Caused by Nitrates in Well Water, Journal of the American Medical Association. 257, 2788-2792.

Cornwell, J.C., Kemp, W.M., Kana, T.M., 1999. Denitrification in coastal ecosystems: methods, environmental controls, and ecosystem level controls: a review. Aquatic Ecology. 33, 41–54.

Dawson, R.F., 1994. Mine waste geotechnics. Ph.D. thesis, Department of Civil Engineering, University of Alberta, Edmonton, AB., 239 pp.

Dawson, R.F., Morgenstern, N.R., Stokes, A.W., 1998. Liquefaction flowslides in Rocky Mountain coal mine waste dumps. Canadian Geotechnical Journal. 35, 328-343.

Durand, P., Breuer. L., Johnes, P., 2011. Nitrogen processes in aquatic ecosystems, in: Sutton, M.A., Howard, C.M., Erisman, J.W., Billen, G., Bleeker, A., Grennfelt, P., Grinsven, H.V., Grizzetti, B. (Eds.), The European Nitrogen Assessment. Cambridge University Press, pp. 126-146.

Egly, R.S., Neckar, A.E., 1964. Ammonium Nitrate-containing Emulsion Sensitizers for Blasting Agents, US Patent No. 3, 161 551.

Eriksson, N., Gupta, A., Destouni, G., 1997. Comparative analysis of laboratory and field tracer tests for investigating preferential flow and transport in mining waste rock. Journal of Hydrology. 194, 143–163.

Essilfie-Dughan, J., Hendry, M. J., Dynes, J., Hu, Y., Biswas, A., 2016. Distribution of sulfur and iron in coal waste rock, Elk Valley, British Columbia, Canada. Int. J. Coal Geol. (*Under Review*).

Ferguson, K.D, Leask, S.M., 1988. The Export of Nutrients from Surface Coal Mines. Regional Program Report 87-12. Environmental Protection, Conservation and Protection, Pacific and Yukon Region, Environment Canada, West Vancouver, B.C., 127 pp.

Focht, D.D., Verstraete, W., 1977. Biochemical ecology of nitrification and denitrification, in: Alexander., M. (Eds.), Advances in Microbial Ecology. Plenum Press, New York, 1, pp. 135-214.

Fukada, T., Hiscock, K.M., Dennis, P.F., Grischek, T., 2003. A dual isotope approach to identify denitrification in groundwater at a river bank infiltration site. Water Research. 37, 3070–3078.

Gibson, D.W., Hughes, J.D., 1981. Structure, stratigraphy, sedimentary environments and coal deposits of the Jura-Cretaceous Kootenay-Group, Crowsnest Pass area, Alberta and British Columbia: field guides to geology and mineral deposits. Geological Association of Canada Annual Meeting, Calgary, AB., 39 pp.

Golder Associates, 2013. Valley-Wide Selenium Management Action Plan for Teck Coal Limited Operations in the Elk Valley: Appendix C- Water Quality Modelling Methods and Calibration. Draft Report; Golder Associates: Calgary, Alberta, Canada.

Goodarzi, F., Huggins, F.E., Sanei, H., 2008. Assessment of elements, speciation of As, Cr, Ni and emitted Hg for a Canadian power plant burning bituminous coal. Int. J. Coal Geology. 74, 1-12.

Hallberg, G.R., Follet, R.F., 1989. Nitrate in ground water in the United States, in: Follett, R. F. (Eds.), Nitrogen Management and Ground Water Protection. Elsevier Science, Amsterdam, Netherlands, pp. 35-74.

Hautman D.P., Munch, D.J., 1997. Environmental Protection Agency Method 300.1, Revision 1.0: Determination of inorganic anions drinking water by ion chromatography. Cincinnati, OHIO: United States Environmental Protection Agency. 40 pp.

Hollocher, T.C., 1984. Source of the oxygen atoms of nitrate in the oxidation of nitrite by Nitrocacter agilis and evidence against a P-O-N anhydride mechanism in oxidative phosphorylation. Archives of Biochemistry and Biophysics. 233, 721-727.

Health Canada, 2014. Guidelines for Canadian Drinking Water Quality—Summary Table. Water and Air Quality Bureau, Healthy Environments and Consumer Safety Branch, Health Canada, Ottawa, ON, 25 pp.

Hendry, J. M., Biswas, A., Essilfie-Dughan, J., Chen, N., Day, S. J., Barbour, S. L., 2015. Reservoirs of selenium in coal waste rock: Elk Valley, British Columbia, Canada, Environmental Science Technology. 49, 8228-8236.

Hendry, M. J., Barbour, S. L., Novakowski, K., Wassenaar, L. I., 2013. Palaeohydrogeology of the Cretaceous Sediments of the Williston Basin using Stable Isotopes of Water. Water Resources Research. 49, 4580–4592.

Horibe, Y., Shigehara, K., Takakuwa, Y., 1973. Isotope separation factors of carbon dioxide-water system and isotopic composition of atmospheric oxygen. Journal of Geophysical Research. 78, 2625-2629.

Hubner, H., 1986. Isotope effects of nitrogen in the soil and biosphere, in: Fritz, P., Fontes, J.C. (Eds.), Handbook of Environmental Isotope Geochemistry: The Terrestrial Environment. Elsevier, Amsterdam, pp. 361–425.

James, C., Fisher, J., Russell, V., Collings, S., Moss, B., 2005. Nitrate availability and hydrophyte species richness in shallow lakes. Freshwater Biology. 50, 1049–1063.

Jeppesen, E., Sondergaard, M., Jensen, J. P., Havens, K. E., Anneville, O., Carvalho, L., Coveney, M. F., Deneke, R., Dokulil, M. T., Foy, B., Gerdeaux, D., Hampton, S. E., Hilt, S., Kangur, K., Kohler, J., Lammens, E. H. H. R., Lauridsen,T. L., Manca, M., Miracle, M. R., Moss, B., Noges, P., Persson, G., Phillips, G., Portielje, R., Romo, S., Schelske, C. L., Straile, D., Tatrai, I., Willen, E. & Winder, M., 2005. Lake responses to reduced nutrient loading—an analysis of contemporary long-term data from 35 case studies. Freshwater Biology. 50, 1747–1771.

Johnson, C. J., Bonrud, P. A., Dosch, T. L., Kilness, A. W., Senger, K. A., Busch, D. C., Meyer, M. R., 1987. Fatal Outcome of Methemoglobinemia in an Infant, Journal of the American Medical Association. 257, 2796-2797.

Kendall, C., 1998. Tracing nitrogen sources and cycling in catchments, in: Kendall, C., McDonnell, J.J. (Eds.), Isotope Tracers in Catchment Hydrology. Elsevier, Amsterdam, pp. 521–576.

Kellman, L., Hillaire-Marcel, C., 1998. Nitrate cycling in streams using natural abundances of to NO_3^- - $\delta^{15}N$ measure in-site denitrification. Biogeochemistry. 43, 273-292.

Killham, K., 1986. Heterotrophic nitrification, in: Prosser, J.I. (Eds.), Nitrification: Special publications of the society for general microbiology. IRL Press, Oxford, pp. 117-126.

Kohl, D.H., Shearer, G.B., Commoner, B., 1971. Fertilizer nitrogen: condition to nitrate in surface water in a corn belt watershed. Science. 174, 1331-1334.

Korom, S.F., Schlag, A.J., Schuh, W.M., Schlag, A.K., 2005. In situ mesocosms: denitrification in the Elk Valley aquifer. Ground Water Monitoring and Remediation. 25, 79-89.

Korom, S.F., Schuh, W.M., Tesfay, T., Spencer, E.J., 2012. Aquifer denitrification and in situ mesocosms: modeling electron donor contributions and measuring rates. Journal of Hydrology, 432-433, 112-126.

Kreitler, C.W., 1979. Nitrogen-isotope ratio studies of soils and groundwater nitrate from alluvial fan aquifers in Texas. Journal of Hydrology. 42, 147-170.

Kroopnick, P., Craig, H., 1972. Atmospheric oxygen: isotopic composition and solubility fractionation. Science. 175, 54–55.

Kross, B.C., Hallberg, G.R., Bruner, R., Cherryholmes, K., Johnson, K.J., 1993. The Nitrate Contamination of Private Well Water in Iowa. American Journal of Public Health. 83, 270-272.

Lehmann, M. F., Reichert, P., Bernasconi, S. M., Barbieri, A., McKenzie, J. A., 2003. Modelling nitrogen and oxygen isotope fractionation during denitrification in a lacustrine redox-transition zone. Geochim.Cosmochim. Acta. 67, 2529−2542.

Macko, S.A., Ostrom, N.E., 1994. Pollution studies using stable isotopes, in: Lajtha, K., Michener, R.H. (Eds.), Stable Isotopes in Ecology and Environmental Science. Blackwell Scientific Publications Oxford, pp. 45-62.

Mariotti, A., Germon, J. C., Hubert, P., Kaiser , P., Letolle, R., Tardieux, A., Tardieux, P., 1981. Experimental determination of nitrogen kinetic isotope fractionation: Some principles; illustration for the denitrification and nitrification processes. Plant and Soil. 62, 413-430.

Mayer, B., Boyer, E.W., Goodale, C., Jaworski, N.A., Breemen, N.V., Howarth, R.W., Seitzinger, S., Billen, G., Lajtha, K., Nadelhoffer, K., Dam, D.V., Hetling, L.J., Nosal, M., Paustian, K., 2002. Sources of nitrate in rivers draining sixteen watersheds in the northeastern U.S.: isotopic constraints. Biogeochemistry. 57, 171–197.

McDonald, L.E., 1987. The Impact of Surface Coal Mining and Municipal Sewage Discharges on Nutrients and Algal Growth in the Elk River Basin, 73 pp.

MEND, 2009. Prediction manual for drainage chemistry from sulphidic geologic materials, Smithers, BC., 597 pp.

Morin, K. A., Gerencher, E., Jones, C. E., Konasewich, D. E., 1991. Critical literature review of acid drainage from waste rock, MEND Report 1.11.1.

Neuner, M., Smith, L., Blowes, D.W., Sego, D.C., Smith, L.J.D., Fretz, N., Gupton, M., 2013. The Diavik waste rock project: water flow though mine waste rock in a permafrost terrain. Applied Geochemistry. 26, 222–233.

Nicholson V., Gillham R.W., Cherry, J.A., Reardon, E.J., 1989. Reduction of acid generation in Mine tailings Through the use of moisture-retaining cover layers as oxygen barriers. Canadian Geotechnical Journal. 26, 1–8.

Nichol, C., Smith, L., Beckie, R., 2005. Field-scale experiments of unsaturated flow and solute transport in a heterogeneous porous medium. Water Resources Research. 41, 1–11.

Nordin, R.N., Pommen, L.W., 2009. Overview Report Update: Water Quality Guideline for Nitrogen (Nitrate, Nitrite, and Ammonia). B.C. Ministry of Water, Land and Air Protection. Canada, 29 pp.

Oremland, R.S., Hollibaugh, J.T., Maest, A.S., Presser, T.S., Miller, L.G., Culbertson, C.W., 1989. Selenate reduction to elemental selenium by anaerobic bacteria in sediments and culture: biogeochemical significance of a novel, sulfate-independent respiration. Applied and Environmental Microbiology. 559, 2333-2343.

Oremland R. S., Steinberg N. A., Maest, A. S., Hollibaugh, J. T., 1990. Measurement of in situ rates of selenate removal by dissimilatory bacterial reduction in sediments. Environmental Science and Technology. 24, 1157–1164.

Oremland, R.S., Steinberg, N.A., Presser, T.S., Miller, L.G., 1991. In situ bacterial selenate reduction in the agricultural drainage systems of western Nevada. Applied Environmental Microbiology. 57, 615–617.

Pardo, L.H., Kendall, C., PettRidge, J., Chang, C.C.Y., 2004. Evaluating the source of streamwater nitrate using $d^{15}N$ and $d^{18}O$ in nitrate in two watersheds in New Hampshire, USA. Hydrological Processes. 18, 2699–2712.

Pommen, L. W., 1983. The effect on water quality of explosives use in surface mining. Volume 1: Nitrogen Sources, Water Quality, and Prediction and Management of Impacts. MOE Technical Report 4. British Columbia Ministry of Environment. Victoria, B.C., 149 pp.

Postma, D., Boesen, C., Kristiansen, H., Larsen, F., 1991. Nitrate reduction in an unconfined sandy aquifer: water chemistry, reduction processes, and geochemical modeling. Water Resources Research. 27, 2027–2045.

Power, J.F., Schepers., J.S., 1989. Nitrate contamination of groundwater in North America. Agriculture, Ecosystem & Environment. 26, 165–187.

Preston, T., Owens, N.J.P., 1983. Interfacing an automatic elemental analyzer with an isotope ratio mass-spectrometer – the potential for fully automated total nitrogen and N-15 analysis. Analyst. 108, 971–977.

Werner, R.A., Brand, W.A., 2001. Referencing strategies and techniques in stable isotope ratio analysis. Rapid Communications in Mass Spectrometry. 15, 501-519.

Revey, G.F., 1996. Practical methods to control explosives losses and reduce ammonia and nitrate levels in mine water. Mining Engineering, 61-64.

Rock, L., Ellert, B., 2007. Nitrogen-15 and Oxygen-18 Natural Abundance of Potassium Chloride Extractable Soil Nitrate Using the Denitrifier Method, Soil Science Society of America Journal. 71, 355-361.

Sawyer, C.N., McCarty, P.L., 1967. Chemistry for sanitary engineers. New York; McGraw-Hill; 518 pp.

Sebilo, M., Billen, G., Grably, M., Mariotti, A., 2003. Isotopic composition of nitrate-nitrogen as a marker of riparian and benthic denitrification at the scale of the whole Seine River system. Biogeochemistry. 63, 35–51.

Sebilo, M., Mayer, B., Grably, M., Billiou, D., Mariotti, A., 2004. The use of the ammonium diffusion method for measurements: comparison with others techniques. Environmental Chemistry. 1, 99–103.

Seiler, R.L., Zaugg, S.D., Thomas, J.M., Howcroft, D.L., 1999. Caffeine and pharmaceuticals as indicators of waste water contamination in wells. Groundwater. 37, 405–410.

Seiler, R.L., 2005. Combined use of $\delta^{15}N$ and $\delta^{18}O$ of nitrate and ^{11}B to evaluate nitrate contamination in groundwater. Applied Geochemistry. 20, 1626–1636.

Seitzinger, S. P., 1990. Denitrification in aquatic sediments, in: Revsbech, N. P., Sørensen, J. (Eds.), Denitrification in Soil and Sediment. Plenum Press, New York, pp. 301-322.

Sigman, D.M., Casciotti, K.L., Andreani, M., Barford, C., Galanter, M., Böhlke, J.K., 2001. A bacterial method for the nitrogen isotopic analysis of nitrate in seawater and freshwater. Analytical Chemistry. 73, 4145-4153.

Silva, S.R., Kendall, C., Wilkison, D.H., Ziegler, A.C., Chang, C.C.Y., Avanzino, R.J., 2000. A new method for collection of nitrate from fresh water and the analysis of nitrogen and oxygen isotope ratios. Journal of Hydrology. 228, 22-36.

Sinditskii, V. P., Egorshev, V. Yu., Levshenkov, A. I., Serushkin,V. V., 2005. Ammonium Nitrate: Combustion Mechanism and the Role of Additives. Propellants, Explosives, Pyrotechnics. 30, 269–280.

Sloth, N.P., Nielsen, L.P., Blackburn, T.H., 1992. Nitrification in sediment cores measured with acetylene inhibition. Limnology and Oceanography. 37, 1108-1112.

Smith, R. L., Harvey, R. W., LeBlanc, D. R., 1991. Importance of closely spaced vertical sampling in delineating chemical and microbiological gradients in groundwater studies. Journal of Contaminant Hydrology. 7, 285–300.

Smith, L., Beckie, R., 2003. Hydrologic and geochemical transport processes in mine waste rock, in: Jambor, J.L., Blowes, D.W., Ritchie, A.I.M. (Eds.), Environmental Aspects of Mine Wastes, Short Course, vol. 31. Mineralogical Association of Canada, pp. 51–72.

Stumm, W., Morgan J.J., 1996. Aquatic Chemistry: Chemical Equilibria and Rates in Natural Waters, 3rd ed.Wiley-Interscience, New York.

SRK., 2010. Selenium leach pads as-built report for Teck Coal, Ltd. Vancouver, B.C. 388 pp.
Teck EVWQP Annex D.4, 2014. Elk Valley Water Quality Plan. Geochemical Source Term Inputs and Methods for the Elk Valley Water Quality Planning Model. Sparwood, BC., 51 pp.
Teck Resources Ltd. 2014. Teck Annual Report.

The Strategic Advisory Panel on Selenium Management, 2010. A Strategic Plan for the Management of Selenium at Teck Coal Operations, Panel report. Calgary, Alberta., 233p.

Wakida, F.T., Lerner, D.N., 2005. Non-agricultural sources of groundwater nitrate: a review and case study. Water Research, 39, DOI: 10.1016/j.watres.2004.07.026.

Wassenaar, L.I., 1995. Evaluation of the origin and fate of nitrate in the Abbotsford Aquifer using the isotopes of ^{15}N and ^{18}O in NO_3^- Applied Geochemistry. 10, 391-405.

U.S. Environmental Protection Agency (EPA), 2009. 2009 Edition of the Drinking Water Standards and Health Advisories. EPA 822-R-09-011, Office of Water U.S. Environmental Protection Agency, Washington, DC., 18 pp.

USGS, 2013. Minerals Yearbook, EXPLOSIVES [ADVANCE RELEASE], 6 pp.

Van der Molen, D. T., Portielje, R., Boers, P. C. M., Lijklema, L., 1998. Changes in sediment phosphorus as a result of eutrophication and oligotrophication in Lake Veluwe, The Netherlands. Water Research. 32, 3281-3288.

Vessey, S.J., Bustin, R.M., 2000. Sedimentology of the coal-bearing Mist Mountain Formation, Line Creek, Southern Canadian Cordillera: relation to coal quality. International Journal of Coal Geology. 42,129–158.

Voerkelius, S., Schmidt, H.L., 1990. Natural oxygen and nitrogen isotope abundance of compounds involved in denitrification: Mitteilungen der Deut. Bodenkundlichen Gesselschaft. 60, 364-366.

Vyazovkin, S., Clawson, J. S., Wight, C. A., 2001. Thermal dissociation kinetics of solid and liquid ammonium nitrate. Chem. Mater. 13, 960–966.

Watts, C.A., Ridley, H., Dridge, E.J., Leaver, J.T., Reilly, A.J., Richardson, D.J., Butler, C.S., 2005. Microbial reduction of selenate and nitrate: common themes and variations. Biochemical Society Transactions. 33, 173-175.

Weres, O., Bowman, H.R., Goldstein, A., Smith, E.C., Tsao, L., Harnden, W., 1990. The effect of nitrate and organic matter upon mobility of selenium in groundwater and in a water treatment process. Water, Air, and Soil Pollution. 49, 251-272.

World Heath Organisation, 2004. Guidelines for drinking water quality, 3rd Edition. WHO, Geneva, 133 pp.

Yoshinari, T., Wahlen, M., 1985. Oxygen isotope ratios in N_2O from nitrification at a wastewater treatment facility. Nature. 317, 349-350.

Young, M., 2007. Professional Engineer with BXL Bulk Explosives Ltd. in Calgary, AB.

Xue, D., Botte, J., De Baets, B., Accoe, F., Nestler, A., Taylor, P., Van Cleemput, O., Berglund, M., Boeckx, P., 2009. Present limitations and future prospects of stable isotope methods for nitrate source identification in surface- and groundwater. Water Resources Research. 43, 1159–1170.

Zhao, H.P., Lai, C., Yang, X., Tang, Y., Rittmann, B.E., 2014. Nitrate shaped the selenate-reducing microbial community in a hydrogen-based biofilm reactor. Environmental Science and Technology. 48, 3395-3402.

APPENDIX A

Table A.1: Results of Pearson's chi squared and F test on logarithm of NO_3^--N concentrations from LCO-WLC waste rock and pre-blast rock samples.

Boreholes	Chi Squared Statistics	Chi Critical	F Statistics	F Critical
LCO-WLC-12-02	9.50	11.1	0.60	0.65
LCO-WLC-12-02 (less than 40 m bgs)	5.32	9.49	0.95	1.69
LCO-WLC-12-02 (greater than 40 m bgs)	7.81	0.57	0.32	0.45
LCO-WLC-12-05a	2.79	5.99	0.70	3.47
LCO-WLC-12-05C1	0.50	9.49	0.94	1.75
LCO-WLC-12-05C2	4.54	9.49	0.95	1.70
Pre-blast (MM1306)	0.44	5.99	0.10	0.41